A comparative isotopic study of the biogeochemical cycle of carbon in modern redox-stratified lakes

Robin Havas[a,*], Christophe Thomazo[a,b], Miguel Iniesto[c], Didier Jézéquel[d], David Moreira[c], Rosaluz Tavera[e], Jeanne Caumartin[f], Elodie Muller[f], Purificación López-García[c], Karim Benzerara[f]

[a] Biogéosciences, CNRS, Université de Bourgogne Franche-Comté, 21000 Dijon, France

[b] Institut Universitaire de France, 75005 Paris, France

[c] Ecologie Systématique Evolution, CNRS, Université Paris-Saclay, AgroParisTech, 91190 Gif-sur-Yvette, France

[d] IPGP, CNRS, Université de Paris, 75005 Paris, and UMR CARRTEL, INRAE & USMB, France

[e] Departamento de Ecología y Recursos Naturales, Universidad Nacional Autónoma de México, México

[f] Sorbonne Université, Muséum National d'Histoire Naturelle, CNRS, Institut de Minéralogie, de Physique des Matériaux et de Cosmochimie (IMPMC), 75005 Paris, France.

[*] *Correspondence to*: Robin Havas (robin.havas@gmail.com)

Keywords: Carbon cycle; DIC; POC; isotopic fractionation; Precambrian analogs

Abstract. The carbon cycle is central to the evolution of biogeochemical processes at the surface of the Earth. Understanding the interplay between the C cycle and physico-chemical and biological conditions in ancient times is challenging because of major differences between the modern and the ancient Earth. Notably, the atmosphere was less oxidizing and the oceans were redox-stratified. Here, we characterized and compared the C cycles in four redox-stratified alkaline lakes from Mexico based on the concentrations and isotopic compositions of dissolved inorganic and particulate organic C (DIC and POC). Measurements were performed in both the water columns and surficial bottom sediments with the assessment of their physico-chemical parameters (conductivity, temperature, O_2, Chl. a, turbidity,). The four lakes exhibit a range of DIC concentrations from 7 to 35 mM, following a gradient of alkalinity/salinity. The DIC and sedimentary carbonates isotopic compositions ($\delta^{13}C_{DIC}$, $\delta^{13}C_{Carb}$) also varied correlatively with alkalinity increasing from -4.1 to +2.0 ‰ and -1.5 to +4.7 ‰, respectively. The porewaters $\delta^{13}C_{DIC}$ reaches up to ~10 ‰ in the sediment of one of the lakes. The $\delta^{13}C_{POC}$ varies from -29.0 to -23.5 ‰ in both the water columns and sediments of the four lakes. The depth profiles of $\delta^{13}C_{POC}$, [POC] and C:N of organic matter shows very similar variations among three of the lakes located in the same area. From the inter-comparison of these datasets in four different systems, we identify the impact of external abiotic factors such as the hydrological regime and inorganic C sources which control the alkalinity, carbonate isotopic signatures, and stratification of some of the physico-chemical parameters. We identify the presence of oxygenic photosynthesis and aerobic respiration metabolisms in the four lakes as well as of methanogenesis in the one with extreme porewater $\delta^{13}C_{DIC}$. Anoxygenic photosynthesis and/or chemoautotrophy are also recognized in two of the lakes, but their POC and DIC signatures can be equivocal. Finally, we find that geochemical signatures of OC in the surficial sediments do not always record the same part of the stratified water column and can be altered by early diagenesis, whereas recently deposited carbonates are more consistently recording the lakes oxycline isotopic compositions. Overall, this work highlights how the integration of datasets from multiple environments facilitates our understanding of the processes affecting the C cycle in redox-stratified systems, while showing the versatility of these processes and how they are recorded in the sedimentary archives.

1. INTRODUCTION

The carbon cycle and biogeochemical conditions prevailing at the surface of the Earth are intimately bound through biological (*e.g.* photosynthesis) and geological processes (*e.g.* volcanic degassing, silicate weathering). Accordingly, the analysis of carbon isotopes in the rock record has been used to reconstruct the evolution of the biosphere and oxygenation of the Earth's (*e.g.* Hayes et al., 1989; Karhu and Holland, 1996; Schidlowski, 2001; Bekker et al., 2008). However, because the oceans have been redox-stratified throughout most of the Earth's history (Lyons et al., 2014; Havig et al., 2015; Satkoski et al., 2015), processes affecting the C cycle were likely different from those occurring in most modern, well oxygenated environments. Indeed, while biological processes evolved through time, dominant chemical reactions occurring in a reducing *vs* oxidizing world were likely not the same. These changing conditions could impact the C cycle at diverse scales, starting from the diversity and relative abundance of microbial carbon and energy metabolism (*e.g.* Wang et al., 2016; Iñiguez et al., 2020; Hurley et al., 2021), to larger ecological interactions (*e.g.* Jiao et al., 2010; Close and Henderson, 2020; Klawonn et al., 2021) and global C dynamics (*e.g.* Ridgwell and Arndt, 2015; Ussiri and Lal, 2017). Nonetheless, some modern stratified analogs (anoxic at depth) of early oceans exist, and need to be characterized in order to better understand the C cycle in ancient redox-stratified systems and how it was recorded by the sedimentary archives (*e.g.* Lehmann et al., 2004; Posth et al., 2017; Fulton et al., 2018). To this end, a number of recent studies investigated the C cycle of modern stratified water columns (*e.g.* Crowe et al., 2011; Kuntz et al., 2015; Camacho et al., 2017; Posth et al., 2017; Schiff et al., 2017; Havig et al., 2018; Cadeau et al., 2020; Saini et al., 2021; Petrash et al., 2022), with the clear advantage that many of their bio-geo-physico-chemical parameters could be directly measured, together with the main C reservoirs. However, these investigations of the C cycle in Precambrian analogues usually focus on a single environment instead of integrating views from several systems (*e.g.* Camacho et al., 2017; Schiff et al., 2017).

Here, we propose to describe the C cycle of four modern redox-stratified alkaline crater lakes, located in the trans-Mexican volcanic belt (Ferrari et al., 2012). For this purpose, we measured the concentrations and isotopic compositions of dissolved inorganic carbon (DIC) and particulate organic carbon (POC) throughout the stratified water column of the lakes. In parallel, depth profiles of several physico-chemical parameters as well as trace and major elements concentrations were measured, allowing to pinpoint the main biogeochemical reactions occurring in the water columns and connect them with specific C isotopes signatures. Last, sedimentary organic carbon and carbonates as well as porewater DIC from surficial sediments (~ 10 cm) at the bottom of the lakes were characterized in order to further constrain the main geochemical reactions taking place in the lower water columns and infer on possible exchanges between the sediment and water column reservoirs.

The four lakes share similar geological and climatic contexts but have distinct solution chemistries (Zeyen et al., 2021) – as well as distinct planktonic communities (Iniesto et al., 2022). Overall, their inter-comparison via the same methodology allows to assess the effects of specific physico-chemical and biological parameters on the C cycle. Moreover, they all correspond to closed lakes in endorheic basins (Alcocer, 2021; Zeyen et al., 2021). This facilitates the identification of external environmental constraints (*e.g.* evaporation, C sources) and allows to discuss their influence on processes occurring within the water columns. Accordingly, we start by constraining the main DIC sources and external controls on the alkalinity of the lakes. Then, we describe the influence played by the inter-lake alkalinity gradient on the lakes stratification and inorganic C cycle, and how it is recorded in the

surficial sediments. Then, combining POC and DIC data, we present the sources of organic C to the lakes by describing the main autotrophic reactions occurring in the water columns (*e.g.* oxygenic and anoxygenic photosynthesis). Finally, we discuss the fate of POC, being recycled (*e.g.* via methanogenesis) or deposited in the sediments and focus on how these reactions are recorded (or not) in surficial sediments.

2. SETTING / CONTEXT

2.1. Geology

The four lakes studied here are volcanic maars formed after phreatic, magmatic and phreatomagmatic explosions, in relation with volcanic activity in the Trans-Mexican-Volcanic Belt (TMVB, Fig. 1). TMVB originates from the subduction of the Rivera and Cocos plates beneath the North America plate, resulting in a long and wide (~1000 and 90-230 km, respectively) Neogene volcanic arc spreading across central Mexico (Ferrari et al., 2012). The TMVB harbors a large variety of monogenetic scoria cones and phreatomagmatic vents (maars and tuff-cones) as well as stratovolcanoes, calderas and domes (Carrasco-Núñez et al., 2007; Ferrari et al., 2012; Siebe et al., 2014). Maar crater formation usually occurs when ascending magmas meet water-saturated substrates, leading to successive explosions and excavation of older units (Lorenz, 1986; Carrasco-Núñez et al., 2007; Siebe et al., 2012; Chako Tchamabé et al., 2020).

Three of the studied lakes (Alchichica, Atexcac and La Preciosa) are located in a restricted area (~ 50 km²) of the Serdan-Oriental Basin (SOB) in the easternmost part of the TMVB (Fig. 1). The SOB is a closed intra-montane basin at high altitude (~2300 m), surrounded by the Los Humeros caldera in the north and the Cofre de Perote-Citlatépel volcanic range in the east. The basement is mainly composed of folded and faulted Cretaceous limestones and shales, covered by andesitic to basaltic lava flows (Carrasco-Núñez et al., 2007; Armienta et al., 2008; Chako Tchamabé et al., 2020). The formations of Alchichica and Atexcac craters were dated back to ~ 6-13 ± 5-6 and 330 ± 80 ka, respectively (Table 1; Carrasco-Núñez et al., 2007; Chako Tchamabé et al., 2020). The age of lake La Preciosa is not known. The fourth lake, La Alberca de los Espinos, is located at the margin of the Zacapu tectonic lacustrine basin in the Michoacán-Guanajuato Volcanic Field (MGVF) in the western-central part of the TMVB (Fig. 1). It lies at about 1985 m, mainly on andesitic basement rocks and was dated at ~25 ± 2 ka (Siebe et al., 2012, 2014).

2.2. Climate and limnology

Due to their geographical proximity, lakes from the SOB experience a similar temperate to semi-arid climate (Armienta et al., 2008; Sigala et al., 2017). The present climate of the SOB is dominated by dry conditions as reflected by higher evaporation than precipitation fluxes in Lake Alchichica (~ 1686 *vs* 392 mm/year; Alcocer, 2021). In Alchichica, Atexcac and La Preciosa, this trend is reflected by a drop in their water level evidenced by the emersion of microbialite deposits in these lakes (Fig. S1; Zeyen et al., 2021). This evaporation-dominated climate strongly contributes to the achievement of relatively high lake salinities from 1.2 to 7.9 psu, ranging from sub- to hyposaline. In comparison, La Alberca's climate is temperate to semi-humid and it is a freshwater lake (0.6 psu, Rendon-Lopez, 2008; Sigala et al., 2017).

The four lakes are warm monomictic, *i.e.*, they are stratified throughout most of the year (~ 9 months) and mix once a year when the thermal stratification breaks down in the cold winter (Armienta et al., 2008). They are all "closed lakes" located in an "endorheic" basin (Alcocer, 2021; Zeyen et al., 2021), *i.e.* they have no inflow, outflow nor a connection to other basins through surficial waters such as streams. Overall, water input is only supplied by precipitations and groundwater inflow as evidenced and quantified for Lake Alchichica (Alcocer, 2021 and references therein).

Finally, the four lakes are alkaline (pH ~ 9) but distribute over a gradient of chemical compositions (including alkalinity, salinity and Mg/Ca ratio), interpreted as reflecting varying concentration stages of an initial alkaline dilute water (Table 1; Zeyen et al., 2021). Variations in concentrations stages may be due to different climates (mostly between La Alberca and lakes from the SOB) and more generally, different hydrological regimes. Microbialite deposits are found in all four lakes (Gérard et al., 2013; Saghaï et al., 2016; Iniesto et al., 2021a, 2021b; Zeyen et al., 2021), with an increasing abundance from lower to higher alkaline conditions (Zeyen et al., 2021).

3. METHOD

3.1. Sample Collection

The sediment core from Lake La Preciosa was collected in May 2016. All other samples were collected in May 2019. The depth profiles of several physico-chemical parameters were measured in the water columns of the four lakes using an YSI Exo 2 multi-parameter probe: temperature, pH, ORP (oxidation reduction potential), conductivity, O_2, chlorophyll a, phycocyanin, and turbidity. Precisions for these measurements were 0.01 °C, 0.1 pH unit, 20 mV, 0.001 mS/cm, 0.1 mg/L, 0.01 µg/L, 0.01 µg/L and 2% FTU unit, respectively. The ORP signal was not calibrated before each profile and is thus used to discuss relative variations over a depth profile. Measurements of the aforementioned parameters allowed to pinpoint depths of interest for further chemical and isotopic analyses, notably around the redoxcline of the lakes. Water samples were collected with a Niskin bottle. Particulate matter was collected on pre-combusted (2 h at 490°C) and weighted glass fiber filters (Whatman GF/F, 0.7 µm) and analyzed for particulate organic carbon (POC), major and trace elements. Between 1.5 and 5 L of lake water were filtered before the GF/F filters got clogged. Then, processed solution was filtered again at 0.22 µm with Filtropur S filters (that were pre-rinsed with the lake water filtered at 0.7 µm) for analyses of dissolved inorganic carbon (DIC), major, minor and trace ions.

Sediment cores were collected using a 90 mm Uwitec corer close to the deepest point of each lake's water column (Table 1), where anoxic conditions prevail almost all year long. Cores measured between 20 and 85 cm in length. Slices of about 2-3 cm were cut under anoxic conditions, using a glove bag filled with N_2 (anoxia were monitored using a WTW3630 equipped with a FDO O_2 optode). Interstitial porewater was drained out of the core slices using Rhizons in the glove bag. Sediments were transported back to the laboratory within aluminized foils (Protpack, UK). Sediments were then fully dried in a laboratory anoxic N_2-filled glove box.

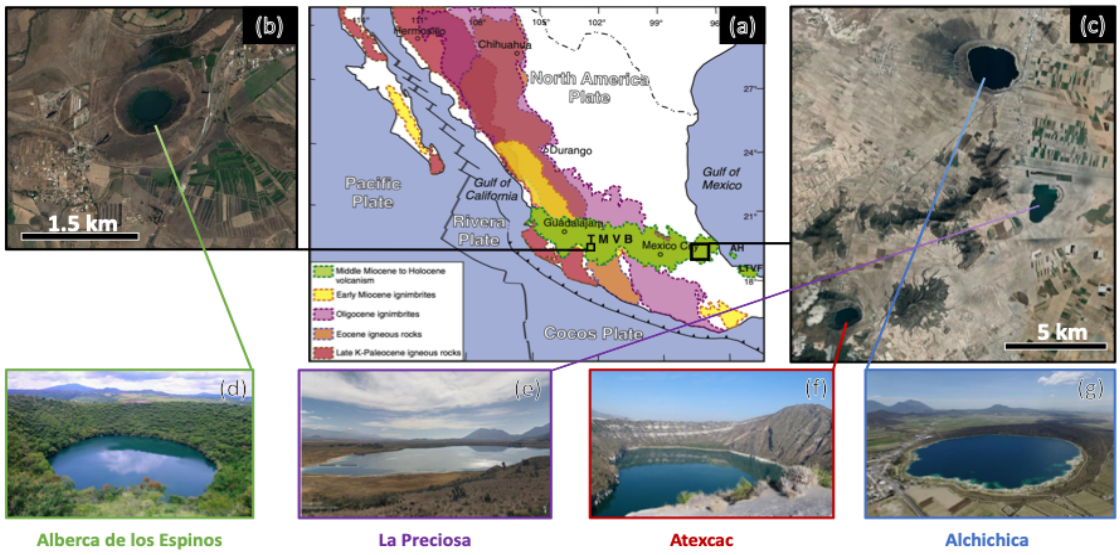

158 Figure 1. Geographical location and photographs of the studied crater lakes. (a) Geological map from Ferrari
159 et al. (2012) representing the location of the four studied lakes in the trans-Mexican volcanic belt (TMVB).
160 (b), (c) Close up © Google Earth views of lake Alberca de los Espinos and the Serdan-Oriental Basin (SOB),
161 respectively. (d-g) Pictures of the four studied lakes (d from © Google Image ['enamoratedemexicowebsite'],
162 e from © Google Earth street view, and g from © 'Agencia Es Imagen').

Lake	General location	Sampling location	Elevation (m.a.s.l.)
Alchichica	Serdan Oriental Basin, eastern TMVB	19°24'51.5" N; 097°24'09.9" W	2320
Atexcac	Serdan Oriental Basin, eastern TMVB	19°20'2.2'' N; 097°26'59.3'' W	2360
La Preciosa	Serdan Oriental Basin, eastern TMVB	19°22'18.1'' N; 097°23'14.4'' W	2330
La Alberca de los Espinos	Zacapu Basin, MGVF, central TMVB	19°54'23.9'' N; 101°46'07.8'' W	1985

163
164

Lake	Lake Basement	Age	Max Depth (m)	Alkalinity (mmol/L)	Salinity (psu)	pH
Alchichica	limestone, basalts	6-13 ± 5-6 ka	63	~35	7.9	9.22
Atexcac	limestone, andesites, basalts	330 ± 80 ka	39	~26	7.4	8.85
La Preciosa	limestone, basalts	Pleistocene	46	~13.5	1.15	9.01
La Alberca de los Espinos	andesite xenoliths	25 ± 2 ka	30	~7	0.6	9.14

165

166 Table 1. General information about the studied lakes. Abbreviations: TMVB: Trans-Mexican volcanic belt;
167 MGVF: Michoaćan-Guanajuato volcanic field; m.a.s.l.: meters above sea level. *NB*: Sampling in May 2019
168 except for La Preciosa's sediments, sampled in May 2016.

3.2. Dissolved inorganic carbon (DIC) concentration and isotope measurements

Twelve milliliters of the 0.7-µm filtered lake water were filtered at 0.22-µm directly into hermetic Exetainer® tubes in order to avoid exchange between DIC and atmospheric CO_2. DIC concentrations and isotopic compositions were measured at the Institut de Physique du Globe de Paris (IPGP, France), using an Analytical Precision 2003 GC-IRMS, running under He-continuous flow, and following the protocol described by Assayag et al. (2006). In short, a given volume of the solution is taken out of the Exetainer® tube with a syringe, while the same volume of helium is introduced in order to maintain a stable pressure and atmospheric-CO_2-free conditions within the sample tubes. The collected sample is introduced in another Exetainer® tube that was pre-filled with a few drops of 100% phosphoric acid (H_3PO_4) and pre-flushed with He gas. Under acidic conditions, the DIC quantitatively converts to gaseous and aqueous CO_2, which equilibrates overnight within the He filled head space of the tube. Quantification and isotopic analyses of released gaseous CO_2 are then carried out by GC-IRMS using internal standards of known composition that were prepared and analyzed via the same protocol. Each measurement represents an average of four injections in the mass spectrometer. Chemical preparation and IRMS analysis were duplicated for all the samples. The $\delta^{13}C_{DIC}$ reproducibility calculated for the 65 samples was better than ±0.2 ‰, including internal and external reproducibility. Standard deviation for [DIC] was 0.6 ± 0.9 mmol/L on average.

Specific DIC speciation, *i.e.*, $CO_{2(aq)}$, HCO_3^- and CO_3^{2-} activities, was computed using Phreeqc with the full dissolved chemical composition of each sample as an input. It should be noted that these results are provided by calculations of theoretical chemical equilibria and do not necessarily take into account local kinetic effects, which, for example, could lead to local exhaustion of $CO_{2(aq)}$ where intense photosynthesis occurs.

3.3. Particulate organic carbon and nitrogen (POC / PON)

Particulate organic matter from the lake water columns was collected on GF/F filters, ground in a ball mill before and after decarbonation. Decarbonation was performed with 12N HCl vapors in a desiccator for 48 h. Aliquots of dry decarbonated samples (25 - 70 mg) were weighed in tin capsules. POC and PON contents and $\delta^{13}C_{POC}$ were determined at the Laboratoire Biogéosciences (Dijon, France) using a Vario MICRO cube elemental analyzer (Elementar, Hanau, Germany) coupled in continuous flow mode with an IsoPrime IRMS (Isoprime, Manchester, UK). USGS 40 and IAEA 600 certified materials were used for calibration and showed a reproducibility better than 0.15 ‰ for $\delta^{13}C$. External reproducibility based on triplicate analyses of samples (n=23) was 0.1 ‰ on average for $\delta^{13}C_{POC}$ (1SD). External reproducibilities of POC and PON concentrations were on average 0.001 and 0.005 mmol/L, respectively (*i.e.* 3 and 7 % of measured concentrations).

3.4. Geochemical characterizations of the sediments

Sedimentary organic carbon (SOC), sedimentary organic nitrogen (SON) and their isotopic compositions were measured on carbonate-free residues of the first 12 cm of the sediment cores, produced after overnight 1N HCl digestion. Plant debris (mainly found in La Alberca and Atexcac) were picked upon initial sediment grinding in an agate mortar and analyzed separately. Aliquots of dried decarbonated samples (~ 4-70 mg) were weighed in tin

capsules. SOC and SON contents and $\delta^{13}C$ were determined at the Laboratoire Biogéosciences (Dijon) using a Vario MICRO cube elemental analyzer (Elementar GmbH, Hanau, Germany) coupled in continuous flow mode with an IsoPrime IRMS (Isoprime, Manchester, UK). USGS 40 and IAEA 600 certified materials were used for calibration and had a reproducibility better than 0.2 ‰ for $\delta^{13}C_{SOC}$. Sample analyses (n=67) were at least duplicated and showed an average external reproducibility of 0.1 ‰ for $\delta^{13}C$ (1SD). External reproducibilities for SOC and SON contents were 0.1 and 0.03 wt. %, respectively.

Carbon isotopic compositions of carbonates from the bottom sediments in La Alberca were analyzed at the Laboratoire Biogéosciences (Dijon) using a ThermoScientific™ Delta V Plus™ IRMS coupled with a Kiel VI carbonate preparation device. External reproducibility was assessed by multiple measurements of NBS19 standard and was better than ± 0.1 ‰ (2σ). Carbonate total concentration was determined by mass balance after decarbonatation for SOC analysis.

Mineralogical assemblages of sediments were determined on bulk powders by X-Ray diffraction (XRD) at the Laboratoire Biogéosciences (Dijon). Samples were ground in an agate mortar. Diffractograms were obtained with a Bruker D8 Endeavor diffractometer with CuKα radiation and LynxEye XE-T detector, under 40 kV and 25 mA intensity. Minerals identification were based on COD ("Crystallography Open Database") and BGMN databases. Estimation of their abundances were achieved using a Rietveld refinement analysis implemented in the Profex software.

Solid sulfide contents were determined on dry bulk sediments in Lake La Alberca after a wet chemical extraction using a boiling acidic Cr(II)-solution as detailed in Gröger et al. (2009).

3.5. Major and trace elements concentrations

Dissolved and particulate matter elemental compositions were measured at the Pôle Spectrométrie Océan (Plouzané, France) by inductively coupled plasma atomic-mass spectroscopy (ICP-AES, Horiba Jobin) for major elements and by high resolution-ICP-mass spectrometry using an Element XR (HR-ICP-MS, Thermo Fisher Scientific) for trace elements. Major element measurement reproducibility based on internal multi-elemental solution was better than 5%. Trace elements were analyzed by a standard-sample bracketing method and calibrated with a multi-elemental solution. Analytical precision for trace elements was generally better than 5%. Dissolved sulfate concentrations were analyzed by ion chromatography at the IPGP (Paris, France) with an uncertainty lower than 5%.

4. RESULTS

4.1. Lake Alchichica

The water column of Lake Alchichica showed a pronounced stratification compared to previous years at the same period (Fig. 2, Fig. S2; Lugo et al., 2000; Adame et al., 2008; Macek et al., 2020). The water temperature varied from about 20 °C at the surface to 15.5 °C at a 30 m depth and below. Dissolved O_2 was slightly oversaturated at the lake surface (112 % or 7.5 mg/L) and rapidly decreased to 0 mg/L between ~ 10 and 20 m depth, while the oxidation reduction potential (ORP) followed a similar trend but decreasing below 30 m. Conductivity hardly

decreased, from 13.8 to 13.7 mS/cm between ~8 and 20 m depth (salinity decreasing from 7.9 to 7.8 psu). Chlorophyll a averaged 2 µg/L, with a broad peak between ~ 7 and 29 m at around 4 µg/L (with a narrow maximum at 6 µg/L at 23 m) and then decreased to minimum values (0.5 µg/L) in the lower water column. pH remained constant at ~9.2 over the whole water column. Based on the temperature profiles, the epi-, meta- and hypolimnion layers of Lake Alchichica in May 2019 extended from 0-10, 10-20 and 20-63 m, respectively (Fig. 2).

Dissolved inorganic carbon (DIC) in the pelagic water column had concentrations comprised between 33 and 35 mM (Fig. 3; Table 2). The $\delta^{13}C_{DIC}$ decreased from 2 to ~ 1.5 ‰ between 5 and 60 m depth (Fig. 4; Table 2). Calculated pCO_2 was about three times higher than the atmospheric pCO_{2atm} (Table S1). Particulate organic carbon (POC) was much smaller with maximum and minimum concentrations of 0.1 mM at 30 m and ~0.02 mM in the bottom part of the water column, respectively. $\delta^{13}C_{POC}$ increased from -26.5 ‰ in the top 30 meters to -24.1 ‰ at 55 m depth. The C:N molar ratio of particulate organic matter (POM) showed a similar profile with values around 10.5 down to 30 m, progressively decreasing towards 5.9 at 55 m (Fig. 3; Table 2).

In the first 12 cm of the sediments, porewater DIC had a concentration (~ 35 mM) and a $\delta^{13}C_{DIC}$ (~ 0 ‰) similar to and slightly lower than the water column values, respectively. Solid carbonates were contained within several phases (aragonite, hydromagnesite, huntite and calcite) and had a bulk C isotopic composition around 4.6 ‰ (Table 3). Sedimentary organic matter had a $\delta^{13}C_{SOC}$ increasing from -25.7 to -24.5 ‰ and constant C:N molar ratio slightly higher than 10 (Figs. 3, 4; Table 3).

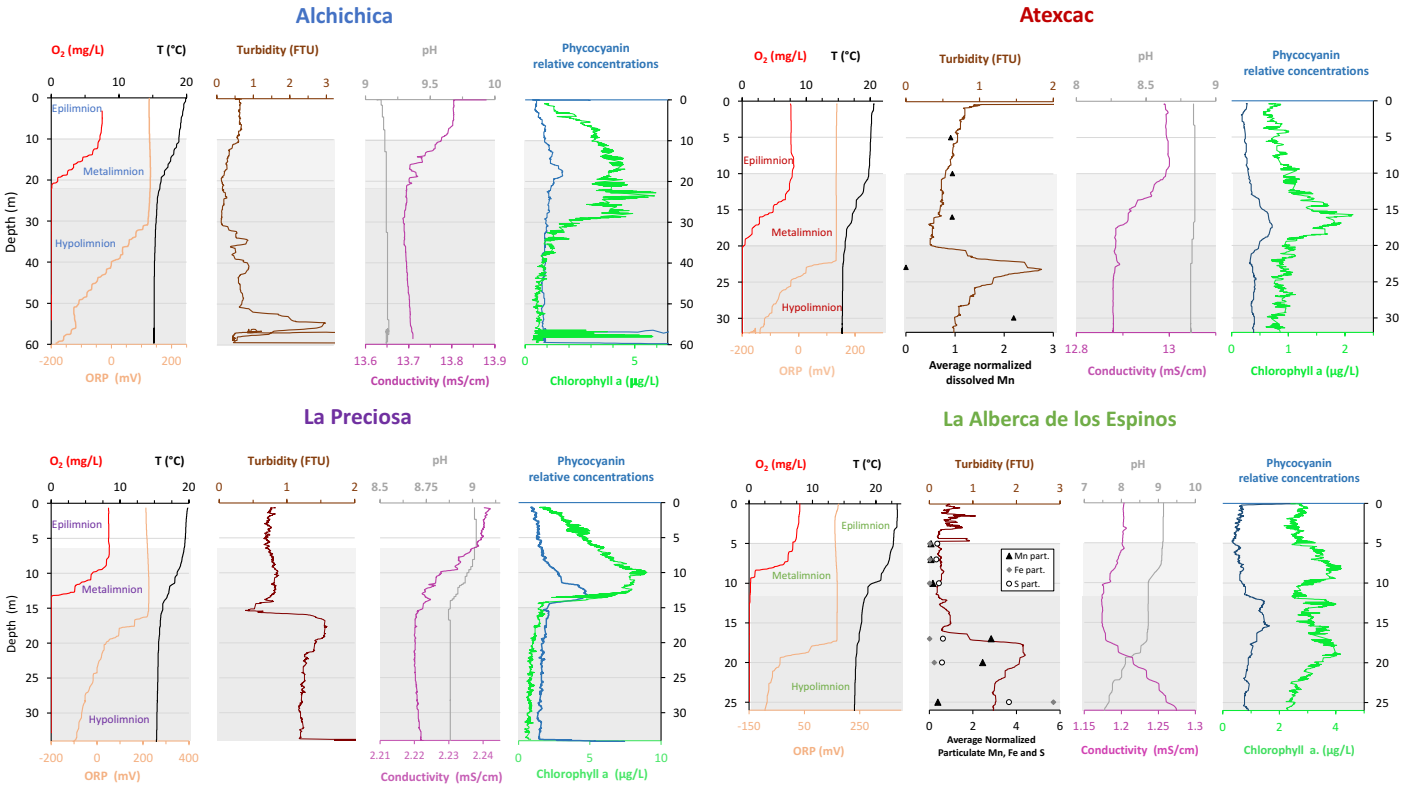

Figure 2. Physico-chemical parameters depth profiles of Alchichica, Atexcac, La Preciosa and Alberca de los Espinos in May 2019 including: dissolved oxygen concentration (mg/L), water temperature (°C), oxidation-reduction potential (ORP, mV), turbidity (Formazin Turbidity Unit), pH, conductivity (mS/cm), phycocyanin and chlorophyll a pigments (µg/L). Absolute values for phycocyanin concentrations were not determined; only relative variations are represented (with increasing concentrations to the right). Discrete concentration values of dissolved Mn in Atexcac and particulate Mn, Fe and S in La Alberca, normalized by their respective average were added. Epi-, meta- and hypo-limnion layers are represented for each lake according to temperature profiles.

4.2. Lake Atexcac

Stratification of the Lake Atexcac water column was also very well defined (Fig. 2). Temperature was about 20.6 °C at the surface and rapidly decreased to 16 °C below 20 m. Conductivity had the same evolution with values around 13 mS/cm near the surface (salinity around 7.4 psu). Dissolved O_2 was also slightly oversaturated at the lake surface (115 % or 7.6 mg/L) and rapidly decreased to 0 mg/L between ~ 10 and 20 m, while ORP signal only decreased below 22 m depth. Chlorophyll a averaged 1 µg/L and showed a narrow peak centered at around 16 m, reaching ~2 µg/L. Turbidity showed a pronounced increase below 20 m, peaking at 23.3 m and returning to surface values at 26 m. Finally, pH remained around 8.85 throughout the water column. Based on the temperature profiles, the epi-, meta- and hypolimnion of Atexcac in May 2019 can be broadly defined as extending from 0-10, 10-20 and 20-39 m, respectively (Fig. 2).

The DIC concentration in the pelagic water column was around 26 mM except at 23 m where it decreased to 24.2 mM (Fig. 3, Table 2). Calculated pCO_2 was about five times higher than the atmospheric pCO_{2atm} (Table S1). The $\delta^{13}C_{DIC}$ was stable around 0.4 ‰ in the epi-/metalimnion but increased to 0.9 ‰ at 23 m and reached minimum values (0.2 ‰) at the bottom of the lake. POC had concentrations of 0.05 mM in the epi-/metalimnion, decreasing to 0.02 mM in the hypolimnion. The C:N molar ratio of POM showed the same depth profile decreasing from ~9.6 in the epi-/metalimnion to 6.6 in the hypolimnion (Fig. 3). $\delta^{13}C_{POC}$ showed minimum values in the epi-/metalimnion (-29.3 ‰ at 16 m) and increased to -26.5 ‰ in the hypolimnion.

Dissolved sulfate concentration was relatively stable at around 2.51 mM throughout the water column but increased to 2.64 mM at 23 m. Dissolved Mn concentration was constant at 1 µM down to 16 m before dropping to 0 at 23 m and increasing again to 2.35 µM at 30 m (Fig. 2; Table S2). This type of profile evolution was also found for other heavy elements such as Cu, Sr, Ba or Pb among others.

In the first 12 cm of the sediments, porewater DIC concentration varied between ~ 21 and 26 mM and $\delta^{13}C_{DIC}$ was around 0 ‰. Carbonates corresponded to aragonite and calcite and had a bulk C isotopic composition comprised between 2.1 and 2.6 ‰ (Table 3). Sedimentary organic matter had a $\delta^{13}C_{SOC}$ around -27 ‰ and a C:N molar ratio increasing from 8 to 10 (Figs. 3, 4; Table 3).

4.3. Lake La Preciosa

Lake La Preciosa was also stratified at the time of sample collection (Fig. 2). The temperature varied from about 20 °C to 16 °C. Conductivity had a similar evolution with values around 2.24 mS/cm near the surface (salinity around 1.15 psu). Dissolved O_2 was oversaturated at the lake surface (120 %, *i.e.*, 8.4 mg/L) and rapidly decreased to 0 between ~ 8 and 14 m, while the ORP decreased right below 16 m. Chlorophyll a concentration averaged 3 µg/L in Lake La Preciosa and recorded the highest peak compared to the other lakes (about 9 µg/L at 10 m) before decreasing to 0.7 µg/L below 15 m. Turbidity showed a large peak between 16 and 19 m. Finally, pH showed a small decrease from 9 to 8.8 between the surface and 15 m depth. Based on the temperature profiles, epi-, meta- and hypolimnion layers of La Preciosa in May 2019 can be broadly defined as extending from 0-6, 6-15 and 15-46 m, respectively (Fig. 2).

The DIC concentration was constant throughout the water column at 13.3 mM, with an exception at 12.5 m, where it decreased to 11.5 mM (Fig. 3, Table 2). Calculated pCO_2 at the surface represented about two times the atmospheric pCO_{2atm} (Table S1). The $\delta^{13}C_{DIC}$ decreased from about 0.5 ‰ to -0.36 ‰ between the surface and the hypolimnion. POC concentration decreased from ~0.06 mM in the epi-/metalimnion to 0.02 mM in the hypolimnion. Similarly, $(C:N)_{POM}$ decreased from ~11.2 in the epi-/metalimnion to 7.6 in the hypolimnion. $\delta^{13}C_{POC}$ increased downward from ~ -27 to -25 ‰ to with a peak to -23.5 ‰ at 15 m.

In the first 10 cm of the sediments, $\delta^{13}C_{SOC}$ values increased downwards from ~ -25.5 to -23.2 ‰ and C:N molar ratio from 9.8 to 11 (Figs. 3, 4; Table 3). Carbonates corresponded to aragonite and calcite and had a bulk C isotopic composition averaging 2.6 ‰ (Table 3). Porewaters from the 2016 La Preciosa core were not retrieved.

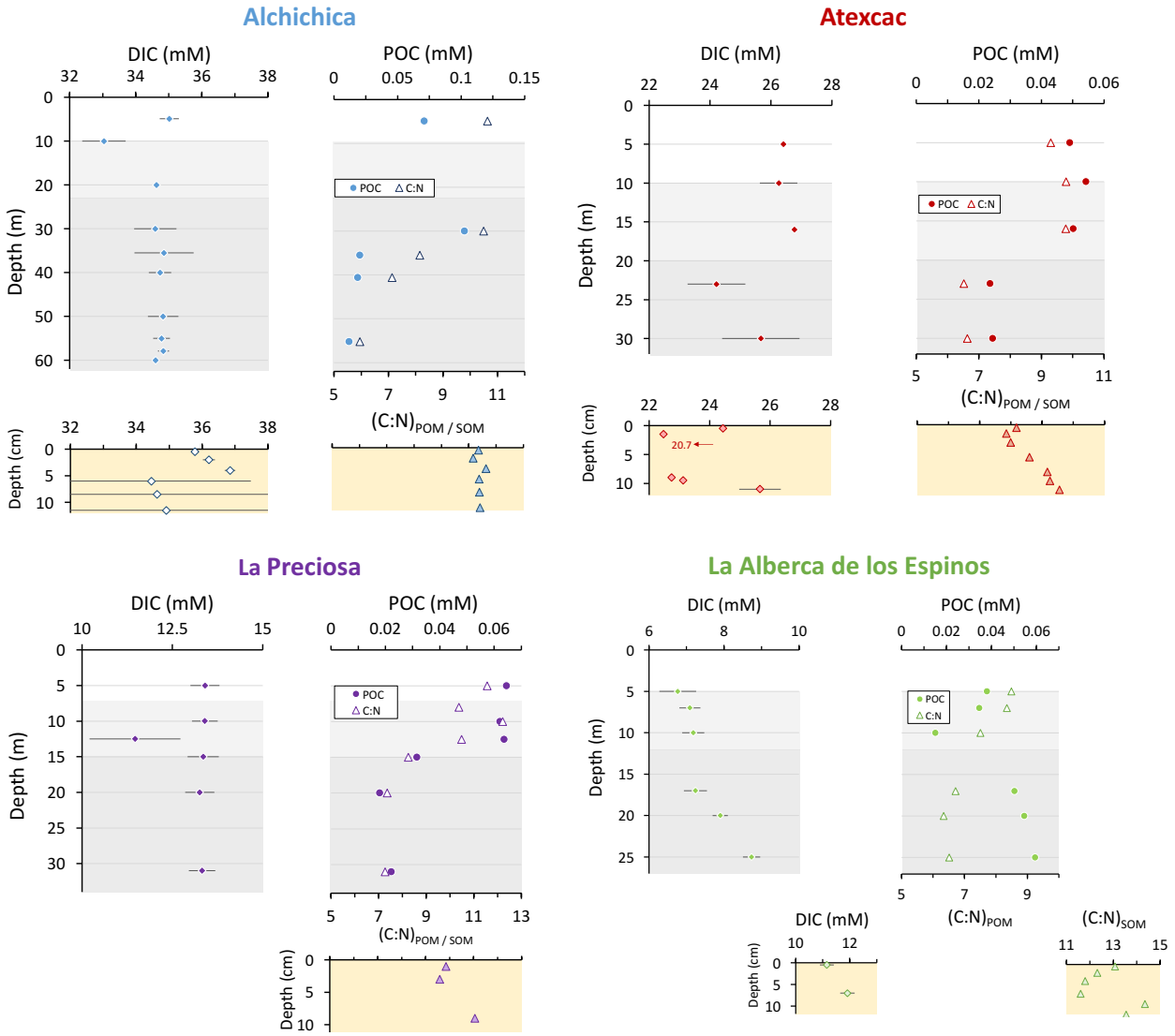

Figure 3. Concentrations in mmol/L (mM) of DIC, DOC, POC and sum of all three reservoirs, C:N molar ratios of POM as a function of depth in the water columns, as well as DIC concentrations in the surficial sediment porewaters and C:N molar ratios of sedimentary OM. Porewaters from La Preciosa's 2016 core were not retrieved.

4.4. Lake La Alberca de los Espinos

Stratification of the water column in La Alberca de los Espinos was also well defined (Fig. 2). Temperature was higher than in the other lakes (evolving from ~23 °C at the surface to 16.5 °C at depth). Dissolved O_2 was

oversaturated at the lake surface (118 %, *i.e.*, 7.9 mg/L) and rapidly decreased to 0 between ~ 5 and 12 m, while the ORP only decreased below 17 m depth. Conductivity decreased from 1.20 to 1.17 mS/cm at 16 m before increasing to 1.27 mS/cm at 26 m (salinity between 0.58 and 0.64 psu). La Alberca had relatively high chlorophyll a levels throughout the water column (3.1 µg/L on average) but showed at least three distinctive peaks, all reaching approximately 4 µg/L. They were found (i) between 6 and 9.5 m, (ii) at around 12.5 m and (iii) between 16 and 19 m. The turbidity profile showed a pronounced increase from 16 to 19 m. The pH showed relatively important variations from 9.15 at the lake surface to 8.75 between 6.5 and 10 m, further decreasing to 7.5 between 16 and 26 m. Based on the temperature profiles, epi-, meta- and hypolimnion layers of Lake La Alberca de los Espinos in May 2019 can be defined as extending from 0-5, 5-12 and 12-30 m, respectively (Fig. 2). Though we notice *via* the conductivity and pH profiles that different conditions prevail at the top and bottom of the hypolimnion.

The DIC concentration progressively increased from 6.8 mM at 5 m to 8.7 mM at 26 m. Calculated pCO_2 at the surface were near equilibrium with atmospheric pCO_{2atm} but strongly increased with depth, up to ~ 40 times pCO_{2atm} (Table S1). The $\delta^{13}C_{DIC}$ first decreased from about -2.5 ‰ to -4.1 ‰ at 10 m, and then increased back, up to -2 ‰ at 25 m. POC concentrations reached minimum values of 0.02 mM at 10 m but increased back to maximum

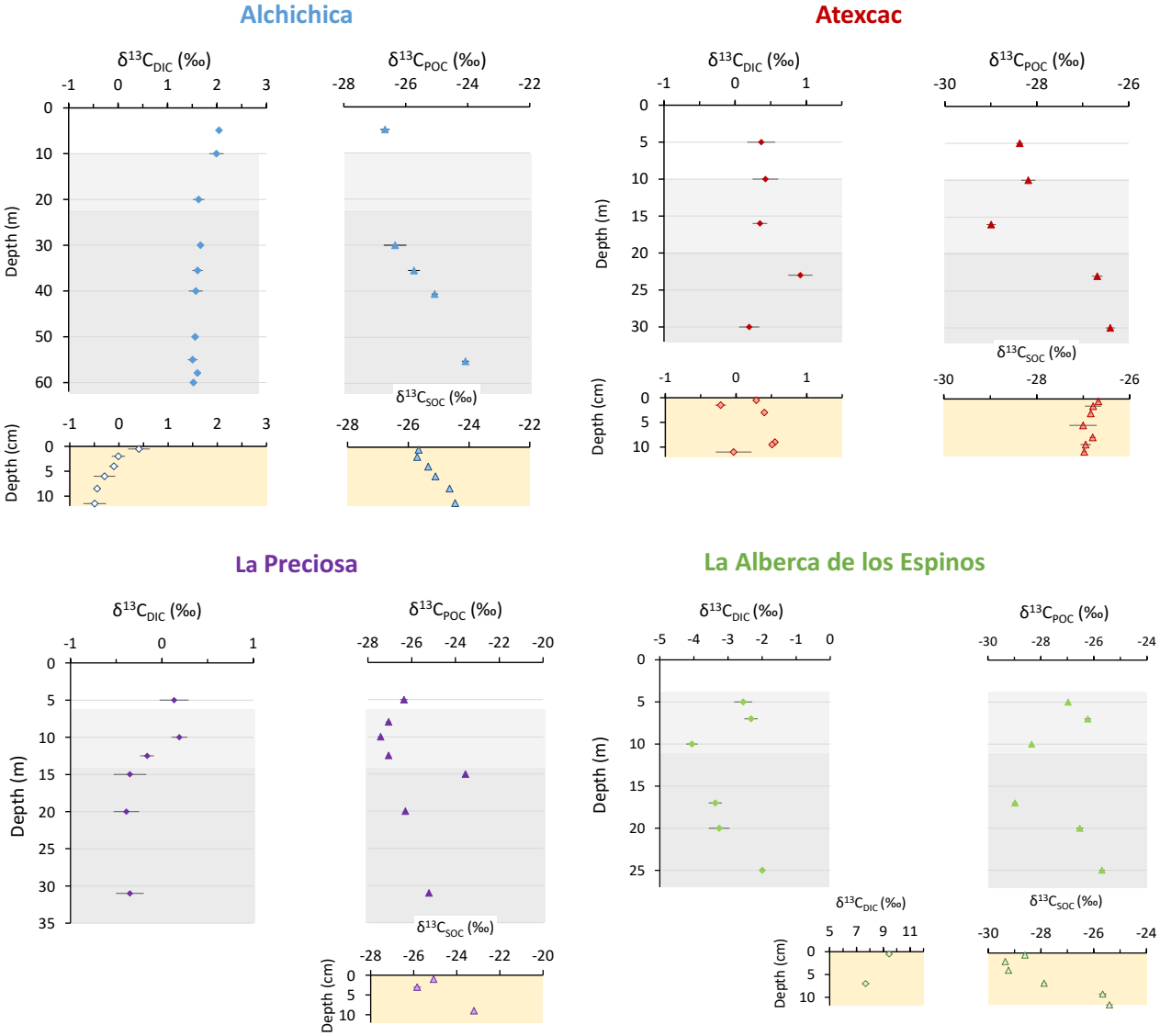

Figure 4. Isotopic compositions of DIC and POC reservoirs as a function of depth in the water columns as well as isotopic compositions of the porewater-DIC and solid organic carbon from the surficial sediments.

values in the hypolimnion (~0.05 mM). The C:N molar ratio of POM progressively decreased from 8.5 at the surface to below 6.5 in the hypolimnion. The $\delta^{13}C_{POC}$ had minimum values at 10 and 17 m (-28.3 and -29 ‰, respectively). Above and below, $\delta^{13}C_{POC}$ was around -26.4 ‰.

Dissolved sulfates as measured by chromatography were only detectable at 5 m with a low concentration of 12 µM, while total dissolved S measured by ICP-AES showed values in the hypolimnion higher than in the upper layers (~ 10.3 *vs.* 7.4 µM, Table S2). Dissolved Mn concentrations decreased from 1.5 to 0.5 µM between 5 and 10 m, then increased to 2 µM at 25 m. Aqueous Fe was only detectable at 25 m with a concentration of 0.23 µM (Table S2). In parallel, particulate S concentrations increased with depth, with a marked increase from 0.1 to 0.6 µM between 20 and 25m. This was spatially correlated with a 25-fold increase in particulate Fe (from 0.2 to 5.97 µM). Particulate Mn showed a peak between 17 and 20 m around 1 µM, contrasting with values lower than 0.15 µM in the rest of the water column (Fig. 2, Table S3).

In the first centimeters of the sediments, porewater DIC concentration and $\delta^{13}C_{DIC}$ varied between ~ 11 and 12 mM and between +8 and +10 ‰, respectively (Figs. 3, 4). Surficial sedimentary carbonates corresponded to calcite and had a $\delta^{13}C$ around -1.5 ‰. Sedimentary organic matter had a $\delta^{13}C_{SOC}$ globally increasing from -29.4 to -25.5 ‰ and a C:N molar ratio varying between 11.6 and 14.3 (Figs. 3, 4; Table 3).

Lake	Sample	DIC	POC	$(C:N)_{POM}$	$\delta^{13}C_{DIC}$	$\delta^{13}C_{POC}$
		mmol/L		(molar)	‰	
Alchichica	AL 5m	35.0	0.07	10.6	2.0	-26.7
	AL 10m	33.0			2.0	
	AL 20m	34.6			1.6	
	AL 30m	34.6	0.10	10.5	1.7	-26.3
	AL 35m	34.9	0.02	8.1	1.6	-25.7
	AL 40m	34.7	0.02	7.1	1.6	-25.1
	AL 50m	34.8			1.6	
	AL 55m	34.8	0.01	5.9	1.5	-24.1
	AL 58m	34.8			1.6	
	AL 60m	34.6			1.5	
Atexcac	ATX 5m	26.4	0.05	9.3	0.4	-28.4
	ATX 10m	26.2	0.05	9.8	0.4	-28.2
	ATX 16m	26.8	0.05	9.8	0.3	-29.0
	ATX 23m	24.2	0.02	6.5	0.9	-26.7
	ATX 30m	25.7	0.02	6.6	0.2	-26.4
La Preciosa	LP 5m	13.4	0.06	11.6	0.1	-26.4
	LP 8m		0.07	10.4		-27.1
	LP 10m	13.4	0.06	12.2	0.2	-27.4
	LP 12.5m	11.5	0.06	10.5	-0.2	-27.1
	LP 15m	13.4	0.03	8.2	-0.3	-23.5
	LP 20m	13.3	0.02	7.4	-0.4	-26.3
	LP 31m	13.3	0.02	7.3	-0.4	-25.2
La Alberca de Los Espinos	Albesp 5m	6.8	0.04	8.5	-2.6	-27.0
	Albesp 7m	7.1	0.03	8.3	-2.3	-26.2
	Albesp 10m	7.2	0.02	7.5	-4.1	-28.3
	Albesp 17m	7.2	0.05	6.7	-3.4	-29.0
	Albesp 20m	7.9	0.05	6.3	-3.3	-26.5
	Albesp 25m	8.7	0.06	6.5	-2.0	-25.7

Table 2. Concentrations and isotopic compositions of dissolved inorganic carbon (DIC) and particulate organic carbon (POC) and C:N molar ratios of particulate organic matter (POM).

5. DISCUSSION

5.1. Inorganic Carbon: origins and implications of the alkalinity/DIC gradient

5.1.1. Sources of DIC and origin of the alkalinity inter-lake gradient

Salinity and DIC gradually increase from Lake La Alberca de los Espinos (~0.6 psu and 7 mM) to Alchichica (~7.9 psu and 35 mM), while lakes La Preciosa and Atexcac have intermediate values of 1.15 and 7.44 psu and 13 and 26 mM, respectively (Table 1 and 2). This matches a gradient of alkalinity (with values of ~ 8, 15, 32 and 47 meq/L, Fig. S3a) previously described for these lakes (Zeyen et al., 2021), consistently with the fact that alkalinity is mostly composed of HCO_3^- and CO_3^{2-} ions in most natural waters. This alkalinity gradient may result from different concentration stages of an initial dilute alkaline water (Zeyen et al., 2021), those different concentration stages being ultimately controlled by the different hydrological regimes of the lakes. First, the weathering of Cretaceous limestone in the SOB (with a $\delta^{13}C$ of approximately 0 ± 1 ‰; Gonzales-Partida et al., 1993; Armstrong-Altrin et al., 2011) together with basaltic/andesitic bedrock (Armienta et al., 2008; Carrasco-Núñez et al., 2007; Lelli et al., 2021) favors the inflow of more alkaline and DIC-concentrated groundwaters than in Lake La Alberca which lies on a essentially basaltic basement (Rendon-Lopez, 2008; Siebe et al., 2014; Zeyen et al., 2021). Second, the SOB area presently experiences higher evaporation than precipitation rates (Alcocer, 2021), probably playing an important role in concentrating solutes and decreasing the water level in lakes Atexcac, Alchichica and La Preciosa (Anderson and Stedmon, 2007; Zeyen et al., 2021). Consistently, substantial "sub-fossil" microbialite deposits emerge above the current water level in lakes Alchichica and Atexcac, evidencing some significant lake level decrease (by up to 15 m in Lake Atexcac, *i.e.* ~40% of today's lake maximum depth; and by about 4 m in Alchichica). Scattered but well emerged patches of microbialites are also found in Lake La Preciosa (suggesting a water level decrease by up to ~5-6 m). By contrast, emerged microbialites are barely observed in Lake La Alberca de los Espinos (Fig. S1).

Additional local parameters, such as varying groundwater paths and fluxes (Furian et al., 2013; Mercedes-Martín et al., 2019; Milesi et al., 2020; Zeyen et al., 2021), most likely play a role in explaining part of the variations in DIC concentration between lakes. For example, Lake La Preciosa's water composition significantly differs from that of lakes Alchichica and Atexcac, despite a similar geological context and climate (all located within 50 km^2, Fig. 1). This could be explained by the fact that groundwaters in the SOB area become more saline as they flow towards the center of the basin and through the crater lakes (Silva Aguilera, 2019; Alcocer, 2021). Since groundwaters flow through La Preciosa first, they are more concentrated as they enter Alchichica than when they enter La Preciosa (Silva Aguilera, 2019; Alcocer, 2021; Lelli et al., 2021). Moreover, distinct regimes of volcanic CO_2 degassing into these crater lakes may also contribute to variations of the C mass balance and $\delta^{13}C_{DIC}$ values between the four lakes. Near the lakes from the SOB area, geothermal fluids derived from meteoric waters interacting with deep volcanic fluids as well as the calcareous basement rocks were evidenced (Peiffer et al., 2018; Lelli et al., 2021). In the water column of Lake La Alberca, the $\delta^{13}C_{total}$ averages -4.8 ‰ (Havas et al., submitted). This is very similar to signatures of mantle-CO_2 (Javoy et al., 1986; Mason et al., 2017) which could buffer the overall C isotopic composition of this lake. A contribution from mantle CO_2 degassing in La Alberca may partially explain the striking increases of P_{CO2} and [DIC] and decrease of pH observed at depth (Table S1; Figs. 2 and 3).

Moreover, this lake is located on top of a likely active normal fault (Siebe et al., 2012), which is favorable to the ascent of volcanic gases.

Last, different remineralization rates of organic carbon could also be a source of heterogeneity between the DIC contents of the lakes. However, assuming that all organic carbon (OC) from the lakes ultimately remineralized into DIC, it would only represent a relatively small portion of the total carbon (16 % in Lake Atexcac, 9 % in Lake La Alberca de los Espinos and ~5 % for lakes Alchichica and La Preciosa; Havas et al., submitted). From an isotopic mass balance perspective, the $\delta^{13}C_{DIC}$ of the three SOB lakes lie very far from OC isotopic signatures, whereas Lake La Alberca exhibits more negative $\delta^{13}C_{DIC}$ (and $\delta^{13}C_{Carb}$), slightly closer to OC signatures (Fig. 4). This latter lake also stands out from the others because of the dense vegetation surrounding it (Fig. S1). Therefore, La Alberca seems to be the only lake where OC respiration could be a significant source of inorganic C to the water column (potentially influencing the P_{CO2}, [DIC] and pH profiles described above).

Lake	Sample name	Depth	$(C:N)_{SOM}$	SOC	$\delta^{13}C_{SOC}$	DIC	$\delta^{13}C_{DIC}$	Carb.	$\delta^{13}C_{Carb}$
		cm	(molar)	wt. %	‰	mmol/L	‰	wt. %	‰
Alchichica	AL19_C2a_01	0-1	10.4	5.1	-25.7	35.8	0.4	41	4.6
	AL19_C2a_02	1-3	10.2	4.7	-25.7	36.2	0.0	44	4.5
	AL19_C2a_03	3-5	10.6	4.3	-25.3	36.8	-0.1	ND.	4.5
	AL19_C2a_04	5-7	10.4	3.8	-25.1	34.5	-0.3	40	4.7
	AL19_C2a_05	7-10	10.4	3.8	-24.6	34.6	-0.4	35	4.5
	AL19_C2a_06	10-13	10.4	3.7	-24.5	34.9	-0.5	38	4.8
Atexcac	ATX19_C1_1	0-1	8.2	0.9	-26.7	24.4	0.3	61	2.5
	ATX19_C1_2	1-2	7.9	1.3	-26.8	22.5	-0.2	46	2.7
	ATX19_C1_3	2-4	8.0	1.1	-26.8	20.7	0.4	61	2.7
	ATX19_C1_S4	4-7	8.6	0.9	-27.0	ND.	ND.	71	2.5
	ATX19_C1_4	7-9	8.7	0.9	-26.8	22.7	0.5	ND.	2.1
	ATX19_C1_5	9-10	9.3	1.0	-26.9	23.1	0.5	64	2.1
	ATX19_C1_S6	10-12	9.6	0.8	-27.0	25.7	0.0	69	2.1
La Preciosa	LP16_C3_7	0-2	9.8	2.3	-25.1	ND.	ND.	61	2.6
	LP16_C3_8	2-4	9.6	2.3	-25.8	ND.	ND.	63	2.6
	LP16_C3_9	8-10	11.0	2.6	-23.2	ND.	ND.	54	2.5
La Alberca de Los Espinos	ALBESP19_C3_1	0-1	13.1	13.3	-28.6	11.2	9.4	20	-1.5
	ALBESP19_C3_2	1-3	12.3	19.0	-29.4	ND.	ND.	18	ND.
	ALBESP19_C3_3	3-5	11.8	16.2	-29.2	ND.	ND.	17	ND.
	ALBESP19_C3_4	5-9	11.6	11.9	-27.9	11.9	7.7	15	-1.5
	ALBESP19_C3_S	9-10	14.3	7.5	-25.7	ND.	ND.	12	ND.
	ALBESP19_C3_5	10-14	13.5	5.4	-25.4	ND.	ND.	12	ND.

Table 3. Analyses of surficial solid sediments and porewaters: sedimentary organic matter C:N ratio; concentrations and isotopic compositions of sedimentary organic carbon (SOC); concentrations and isotopic compositions of DIC in the porewaters and solid bulk carbonates.

397

398 **5.1.2. Influence of the lakes' alkalinity on their physico-chemical stratification features**

399 Stratified water columns can sustain strong physico-chemical gradients, where a wide range of biogeochemical
400 reactions impacting the C cycle can take place (*e.g.* Jézéquel et al., 2016). Here, temperature, conductivity and O_2
401 profiles show that the four lakes were clearly stratified at the time of sampling and had a similar general structure,
402 although depths defining the successive epi-, meta- and hypolimnion layers differed between the lakes (Fig. 2).

403 The evolution of pH with depth exemplifies the interplay between the alkalinity gradient, the physico-chemical
404 stratification of the lakes, and their respective C cycle. pH showed a stratified profile in La Preciosa and La
405 Alberca, whereas it remained constant in Alchichica and Atexcac. The pH decline at the oxycline of Lake La
406 Preciosa was associated with the decrease of POC and chlorophyll a concentrations and $\delta^{13}C_{DIC}$ values, reflecting
407 the impact of oxygen respiration (*i.e.* carbon remineralization) at this depth (Figs. 2-4). In Lake La Alberca, the
408 surface waters are markedly more alkaline than the bottom waters, with a two-step decrease of pH occurring at
409 around 8 m and 17 m (total drop of 1.5 pH unit). Based on the same observations as in La Preciosa, this likely
410 results from high OM respiration, although input of volcanic acidic gases (*e.g.* dissolved CO_2 with $\delta^{13}C \sim -5$ ‰)
411 might also contribute to the pH decrease in the bottom waters, as reflected by negative $\delta^{13}C_{DIC}$ signatures and the
412 increase of [DIC] and conductivity in the hypolimnion (Figs. 2 and 4). By contrast, while the same pieces of
413 evidence for oxygen respiration ([POC], chlorophyll a) can be detected in the two other lakes, this did not similarly
414 impact their pH profile (Fig. 2). This suggests that the acidity generated by these reactions is buffered by the much
415 higher alkalinity measured in these two lakes. Overall, several external forcings such as lake hydrology or fluid
416 sources impact the alkalinity buffering capacity of these lakes. Thereby, they also influence their vertical pH
417 profile, which is particularly important considering the critical interplay between pH and biogeochemical reactions
418 affecting the C cycle (*e.g.* Soetaert et al., 2007).

419

420 **5.1.3. Isotopic signatures of inorganic C in the lakes ($\delta^{13}C_{DIC}$ and $\delta^{13}C_{Carbonates}$)**

421 The DIC isotopic composition of the lakes – between ~ -3 and +2 ‰ on average (Table 2) – is consistent with the
422 DIC sources described above. On one hand, those from the SOB lakes are similar to the estimated value of
423 groundwater $\delta^{13}C_{DIC}$ coming from the alteration of the Cretaceous limestone basement. On the other hand, lower
424 $\delta^{13}C_{DIC}$ in Lake La Alberca is consistent with an influence of remineralized OC and/or volcanic CO_2.

425 By controlling the DIC speciation ($H_2CO_3/CO_{2(aq)}$, HCO_3^-, CO_3^{2-}), pH also strongly influences $\delta^{13}C_{DIC}$ because
426 there is a temperature dependent fractionation of up to ~10 ‰ between the different DIC species (Emrich et al.,
427 1970; Mook et al., 1974; Bade et al., 2004; Table S4). Consistently, the $\delta^{13}C_{DIC}$ of Mexican lakes are in the
428 expected range for lakes with a pH around 9 (Bade et al., 2004), where DIC is dominated by HCO_3^-. However, the
429 pH values of the studied Mexican lakes are too close to each other to explain the significant difference observed
430 between their $\delta^{13}C_{DIC}$ (Fig. 4; p=4.2x10^{-3} for Lakes Atexcac and La Preciosa which have the closest $\delta^{13}C_{DIC}$). Part
431 of the variability of $\delta^{13}C_{DIC}$ among the lakes may result from their varying evaporation stages. This is suggested
432 by the observation that the mean $\delta^{13}C_{DIC}$ values of the lakes broadly correlate with their salinity/alkalinity
433 (Fig. S3b). This relationship is expected as evaporation generally increases the $\delta^{13}C_{DIC}$ of residual waters, notably

because it increases lake pCO_2 and primary productivity which bolsters CO_2 degassing and organic C burial, both having low $\delta^{13}C$ compared to DIC (*e.g.* Li and Ku, 1997; Talbot, 1990). Accordingly, the pCO_2 of La Alberca is smaller than in the other lakes (Table S1). Additionally, slightly higher temperatures recorded in La Alberca's surface waters would make degassing $CO_{2(g)}$ slightly less fractionated towards HCO_3^-/CO_3^{2-} ions (Table S4). Thus, even if the four lakes were characterized by similar CO_2-degassing rates, the increase of DIC isotopic composition related to this process would be smaller for La Alberca's $\delta^{13}C_{DIC}$. Lastly, lakes with lower DIC concentrations are expected to have a $\delta^{13}C_{DIC}$ more easily influenced by exchanges with other carbon reservoirs, such as organic carbon (through photosynthesis/respiration) or other DIC sources (*e.g.*, depleted volcanic CO_2 or groundwater DIC) – compared with buffered, high DIC lakes (Li and Ku, 1997). Consistently, low DIC/alkalinity concentration in Lake La Alberca corresponds to the lowest $\delta^{13}C_{DIC}$ of the four lakes, likely reflecting organic and/or volcanic C influence, and thus a higher responsiveness to biogeochemical processes of the inorganic C reservoir.

As a result, the isotopic composition of sedimentary carbonates ($\delta^{13}C_{Carb}$) which precipitate from the water column DIC primarily follows the alkalinity gradient trend with the lowest $\delta^{13}C_{Carb}$ found in the surficial sediments of La Alberca (~ -1.5 ‰), the highest values in Alchichica (~ +4.6 ‰) and La Preciosa and Atexcac having intermediate values (around 2.5 ‰) (Table 3). More precisely, we can estimate the $\delta^{13}C_{DIC}$ from which the carbonates precipitated by correcting for the isotopic fractionation existing between different carbonate phases and the lake DIC (supplementary text S1). From this, it appears that surficial sedimentary carbonates are in isotopic equilibrium with the $\delta^{13}C_{DIC}$ of the upper water columns, more specifically from the oxycline/thermocline, except in Lake Atexcac (Tables S4 and S5). In this latter lake, the $\delta^{13}C$ of carbonate precipitation is slightly lower than the $\delta^{13}C_{DIC,}$ possibly related to detrital carbonate inputs from the surrounding microbialites. Thus, some detrital carbonate may contribute to the bulk sediment carbonates and slightly deviate the isotopic record from the theoretical equilibrium fractionation such as observed in Atexcac with a small offset of a few tenth of ‰.

5.1.4. Sinks of DIC along the alkalinity gradient

Interplays between pH and sources of alkalinity/DIC in the lakes also have a strong impact on their C storage capacity as they can result in different fluxes of the C sinks (inorganic and organic C precipitation / sedimentation, CO_2 degassing).

To a first order, alkaline pHs allow a relatively important storage of DIC because they favor the presence of HCO_3^- and CO_3^{2-} species over H_2CO_3* (the intermediate specie between gaseous $CO_{2(g)}$ and the bi-/carbonate ions and defined here as the sum of H_2CO_3 and $CO_{2(aq)}$). In the studied lakes, carbonate and bicarbonate ions represent over 99% of total DIC (Table S1). Nonetheless, large amounts of CO_2 degas out of the surface of lakes Alchichica, Atexcac and La Preciosa, as suggested by their elevated surface water pCO_2, amounting from 2 to 5 times higher the atmospheric pCO_{2atm} (Table S1). Thus, these lakes currently act as CO_2 sources to the atmosphere. Meanwhile, the lake with the lowest DIC (La Alberca de los Espinos) has surface waters in equilibrium or even with lower pCO_2 than pCO_{2atm} (Table S1). These observations are consistent with the idea that higher DIC concentrations favor CO_2 degassing through higher pCO_2 (despite high pH values). For the same pH in the surface waters of lakes Alchichica and La Alberca (the two endmembers of the alkalinity gradient), there is over three times more CO_2 degassing out of Alchichica than La Alberca (for a given value of gas transfer velocity). However, we notice that

most degassing occurs in Lake Atexcac (pCO_{2surf}/pCO_{2atm} = 5 at the moment of sampling; Table S1) due to a lower pH and thus a higher proportion of H_2CO_3*.

Another important sink of C for these lakes is the precipitation of carbonate minerals, composing the microbialites and bottom lake sediments. Here again the respective lake alkalinities and consequent mineral saturation indexes greatly influence the amount of C being precipitated out from the lakes waters. While the four lakes are supersaturated with respect to aragonite, calcite and the precursor phase monohydrocalcite, they show highly contrasting amounts of carbonate deposits (Zeyen et al., 2021). The degree of microbialite occurrence increases along the alkalinity gradient with Alchichica and Atexcac notably harboring massive deposits, whereas La Alberca has limited ones (Zeyen et al., 2021; Fig. S1). Similarly, surficial sediments contain from 40 to 62 wt. % carbonates on average for the SOB lakes but only 16 wt. % for La Alberca (Table 3). Thus, based on this large difference in carbonate precipitate quantities (both in microbialites and bottom sediments), it seems overall that the lakes from the SOB bury more C than Lake La Alberca de los Espinos, although a detailed estimation of these C fluxes (including sedimentation rates, porosity, etc.) would be required to fully constrain this aspect. Nevertheless, based on the data from May 2019, La Alberca was the only of the four lakes to have a pCO_2 in equilibrium with the atmosphere (and not higher) and therefore represents a net sink of C. Classifying the three other lakes as net C sources or sinks – notably in order to see the influence of their respective position in the alkalinity gradient – will require a more detailed description of C in- and out-fluxes since they all store and emit significant amounts of C (as organic and inorganic C deposits and via CO_2 degassing, respectively). However, this is out of the scope of the present study.

In summary, although the four lakes present the same general structure and environmental conditions (*i.e.* being tropical alkaline stratified crater-lakes), external and local factors (such as hydrology, fluid sources or stratification characteristics) result in contrasting compositions of their water chemistries, which in turn, have a critical impact on the physico-chemical depth profiles of each lake and their biogeochemical carbon cycle functioning. Notably, these external factors represent a first order control on the size, the isotopic composition and the responsiveness to biogeochemical processes of the inorganic C reservoir. Interestingly, C storage in mineral carbonates seems to be significant in watersheds where carbonate deposits already pre-exist in the geological substratum (here the Cretaceous limestone basement), providing more alkaline and C-rich sources.

Symbols	Mathematical Expression	Signification
$\delta^{13}C_X$	$\left(\frac{\left(\frac{^{13}C}{^{12}C}\right)_X}{\left(\frac{^{13}C}{^{12}C}\right)_{\dots}} - 1\right) * 1000$	Relative difference in ^{13}C:^{12}C isotopic ratio between a sample of a given C reservoir and the international standard "Vienna Pee Dee Bee", expressed in permil (‰). $\delta^{13}C_{total}$ represents the weighted average of $\delta^{13}C$ for all DIC and POC.
$\Delta^{13}C_{X\text{-}Y}$	$= \delta^{13}C_X - \delta^{13}C_Y \approx 1000 ln \alpha_{X\text{-}Y}$	Apparent isotopic fractionation between two reservoirs 'X' and 'Y'. Difference between their measured C isotope compositions approximating the fractionation α in ‰.
$\varepsilon_{X\text{-}CO2}$	$= (\alpha_{X\text{-}CO2} - 1)1000 \approx \delta^{13}C_X - \delta^{13}C_{CO2}$	Calculated isotopic fractionation between a reservoir 'X' and $CO_{2(aq)}$. $\alpha_{X\text{-}CO2}$ is calculated as $(\delta^{13}C_X+1000)/(\delta^{13}C_{CO2}+1000)$ where $\delta^{13}C_X$ is measured and $\delta^{13}C_{CO2}$ is computed based on DIC isotopic composition and speciation (see supplementary text S1).

Table 4

Index for mathematical notations used in the text including C isotopic composition of a reservoir X ($\delta^{13}C_X$), isotopic discrimination between the two carbon reservoirs X and Y ($\Delta^{13}C_{X\text{-}Y}$). In the main text, we report organic C isotopic discrimination *versus* both bulk DIC ($\Delta^{13}C_{POC\text{-}DIC}$) – in a way to facilitate studies intercomparison and because it is the commonly reported raw measured data (Fry, 1996) – and calculated $CO_{2(aq)}$ ($\varepsilon_{POC\text{-}CO2}$) in order to discuss the intrinsic isotopic fractionations associated with the lakes metabolic diversity. All C isotope values and fractionations are reported relative to the international standard VPDB (Vienna Pee Dee Belemnite).

5.2. Particulate organic carbon: from water column primary production to respiration recycling and sedimentary organic matter

5.2.1. Particulate organic C sources

Primary productivity by oxygenic photosynthesis in the upper water column

All four crater lakes are endorheic basins, *i.e.* there is no surface water inflow or outflow. Therefore, the organic carbon sources are predominantly autochthonous, mainly resulting from planktonic autotrophic C fixation. This is supported by C:N ratios of POM that were comprised between 6 and 12 in the four lakes, *i.e.*, close to the phytoplankton Redfield but far from land plant ratios. Abundant vegetation covers the crater walls of Lake La Alberca and to a lesser extent Lake Atexcac; some plant debris were observed and sampled in the sediment cores of these two lakes. They had high C:N ratios (between 24 and 68), typical of plant tissues and significantly higher than those of the bulk organic matter of surficial sediments (between 8 and 13) and the water column (between 6 and 12) (Fig. 3). Therefore, allochthonous organic carbon in these two lakes – albeit present – does not significantly contribute to their bulk organic signal.

The importance of planktonic autotrophic C fixation as a major source of organic C in the four lakes is further supported by the assessment of the isotopic discrimination between DIC and organic biomass, expressed as $\Delta^{13}C_{POC\text{-}DIC}$ and $\varepsilon_{POC\text{-}CO2}$ (Table 4). The $\Delta^{13}C_{POC\text{-}DIC}$ vary between ~ -29 and -23 ‰ (corresponding to $\varepsilon_{POC\text{-}CO2}$ between ~ -19 and -13 ‰; Table 5) throughout the four water columns, which is in the typical range of planktonic oxygenic phototrophs (Pardue et al., 1976; Sirevag et al., 1977; Thomas et al., 2019). Yet, these values exhibit variability – both within a single water column (up to 4.5 ‰) and between the different lakes (up to 6 ‰, Figs. 4 and 5). This variability may trace several abiotic and biotic factors.

Notably, higher DIC availability in Alchichica and Atexcac probably makes the carboxylation step more limiting during photosynthesis (*e.g.* O'Leary, 1988; Descolas-Gros and Fontungne, 1990; Fry, 1996), increasing $|\varepsilon_{POC\text{-}CO2}|$ in these lakes (between 17.5 and 19.2 ‰ at the peak of Chl. a) compared to La Preciosa and Alberca (Fig. 5a; between 14.5 and 17.7 ‰). Indeed, lower $CO_{2(aq)}$ availability and/or higher reaction rates result in transport-limited rather than carboxylation-limited fixation and thus, smaller C isotope fractionation between POC and DIC (Pardue et al., 1976; Zohary et al., 1994; Fry, 1996; Close and Henderson, 2020). This is because the isotopic fractionation associated with diffusion is much smaller than with carboxylation and because a higher proportion of the DIC entering the cells is converted into organic biomass (*e.g.* Fogel and Cifuentes, 1993). Consistently, we notice a correlation among the lakes between $a(CO_2)_{(aq)}$ (or [DIC]) and $|\varepsilon_{POC\text{-}CO2}|$ at depths where oxygenic photosynthetic peaks (Fig. 6). Furthermore, lakes La Preciosa and Alberca are considered less oligotrophic than the two other lakes (Lugo et al., 1993; Vilaclara et al., 1993; Havas et al., submitted), consistently with higher chlorophyll a contents and thus smaller $|\varepsilon_{POC\text{-}CO2}|$ (Fig. 5). Last, higher water temperatures in La Alberca de los Espinos (by ~ 3 °C) could partly contribute to a smaller $|\varepsilon_{POC\text{-}CO2}|$ in this lake (Sackett et al., 1965; Pardue et al., 1976; Descolas-Gros and Fontungne, 1990).

Unlike $\delta^{13}C_{DIC}$, organic carbon isotopic signatures do not evolve linearly with the alkalinity/salinity gradient, suggesting other lake- and microbial-specific controls on these signatures. These controls include: diffusive or active uptake mechanisms, specific carbon fixation pathways, the fraction of intracellular inorganic carbon

released out of the cells, cell size and geometry (Werne and Hollander, 2004 and references therein) and remineralization efficiency. Moreover, an increasing number of isotopic data has evidenced a significant variability of the isotopic fractionation achieved by different purified RuBisCO enzymes ($\varepsilon_{RuBisCO}$, Iñiguez et al., 2020), and even by a single RuBisCO form (Thomas et al., 2019). Thus, caution should be paid to the interpretation of the origin of small isotopic variations of the biomass in distinct environmental contexts because RuBisCO alone can be an important source of this variability (Thomas et al., 2019).

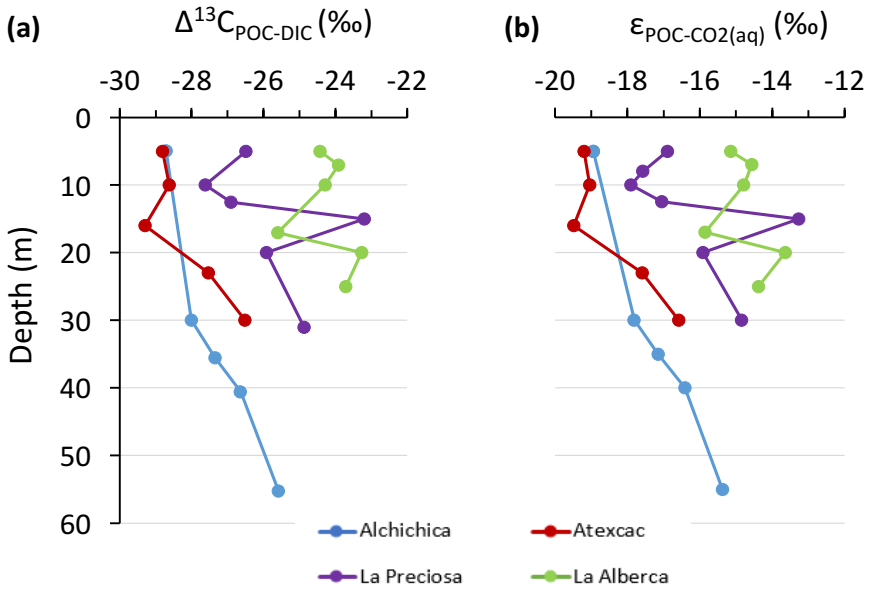

Figure 5.

Isotopic fractionations between POC and DIC in the water columns of the four lakes, expressed as a) $\Delta^{13}C_{x\text{-}y}$ and b) $\varepsilon_{POC\text{-}CO2}$. Refer to Table 4 for more detail about the Δ and ε notations.

Lake	Sample	$\Delta^{13}C_{POC\text{-}DIC}$	$\varepsilon_{POC\text{-}CO2}$
		‰	
Alchichica	AL 5m	-28.7	-18.7
	AL 30m	-28.0	-17.5
	AL 35m	-27.3	-16.9
	AL 40m	-26.6	-16.1
	AL 55m	-25.6	-15.1
Atexcac	ATX 5m	-28.8	-18.9
	ATX 10m	-28.6	-18.8
	ATX 16m	-29.3	-19.2
	ATX 23m	-27.5	-17.3
	ATX 30m	-26.5	-16.3
La Preciosa	LP 5m	-26.5	-16.7
	LP 10m	-27.6	-17.7
	LP 12.5m	-26.9	-16.9
	LP 15m	-23.2	-13.1
	LP 20m	-25.9	-15.8
	LP 31m	-24.9	-14.7
La Alberca de Los Espinos	Albesp 5m	-24.4	-15.0
	Albesp 7m	-23.9	-14.5
	Albesp 10m	-24.3	-14.7
	Albesp 17m	-25.6	-15.8
	Albesp 20m	-23.3	-13.6
	Albesp 25m	-23.7	-14.4

Table 5

Isotopic fractionations between dissolved inorganic carbon (DIC) and particulate organic carbon (POC). $\Delta^{13}C_{POC\text{-}DIC} = \delta^{13}C_{POC} - \delta^{13}C_{DIC}$ is the apparent fractionation and ε is computed as the actual metabolic isotopic discrimination between CO_2 and POC (see Table 4). The full chemistry of lake Alchichica sample at 35 m depth was not determined, thus, calculation of $\delta^{13}C_{CO2}$ for this sample was based on the composition of samples beneath and above.

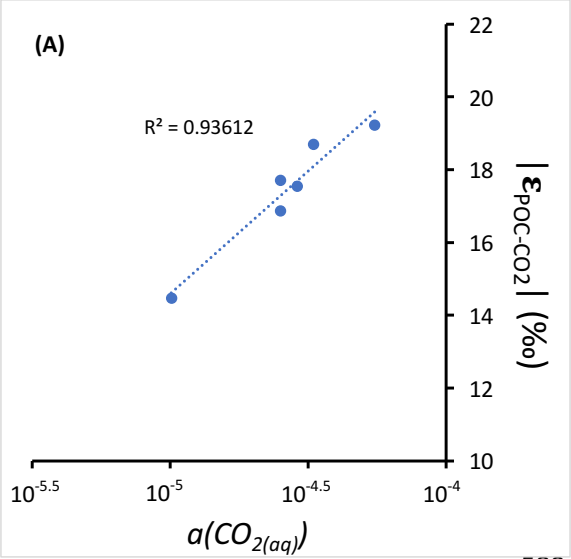

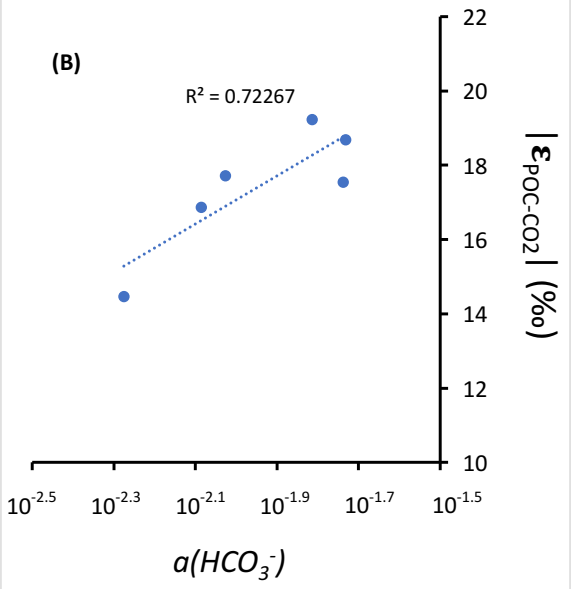

Figure 6.

Cross plots of DIC species activities *versus* absolute values of calculated C isotopic fractionations between POC and CO_2 at depths of peak oxygenic photosynthesis where data was available (5 and 30 m for Alchichica, 16 m for Atexcac, 10 and 12.5 m for La Preciosa and 7 m for La Alberca). (A) Dissolved $CO_{2(aq)}$ activity and (B) bicarbonate activity as functions of $|\varepsilon_{POC\text{-}CO2}|$ in ‰ plus linear correlation trends and corresponding R^2.

Anoxygenic autotrophs commonly thrive in anoxic bottom waters of stratified water bodies (*e.g.* (Pimenov et al., 2008; Zyakun et al., 2009; Posth et al., 2017; Fulton et al., 2018; Havig et al., 2018). Consistently, they have been identified at different depths in the four Mexican lakes (Macek et al., 2020; Iniesto et al., 2022). Based on our results obtained on samples collected during the stratification period, anoxygenic autotrophs appear to have a distinctive impact on the C cycle of lakes Atexcac and La Alberca only. Indeed, Lake Atexcac records a concomitant decrease of [DIC] and increase of $\delta^{13}C_{DIC}$ in the anoxic hypolimnion at 23 m, below the peak of chlorophyll a, suggesting autotrophic C fixation by chemoautotrophy or anoxygenic photosynthesis. The calculated $\varepsilon_{POC\text{-}CO2}$ at 23 m (-17.3 ‰) is consistent with C isotopes fractionation by purple- and green-sulfur-anoxygenic bacteria (PSB and GSB), while $\varepsilon_{POC\text{-}CO2}$ in La Alberca's hypolimnion (~ -15 ‰) is closer to GSB canonical signatures (Posth et al., 2017 and references therein) (Fig. 5b). In La Alberca, anoxygenic primary productivity is moreover suggested by increasing POC concentrations below the oxycline. Besides, we also observe a Chl. a peak in the anoxic hypolimnion of this lake (Fig. 2), which likely represents a bias of the probe towards some bacteriochlorophylls typical of GSB (see supplementary text S3). We notice that in Lake Atexcac, C fixation at 23 m by anoxygenic autotrophs causes a shift in the DIC reservoir, while oxygenic photosynthesis at 16 m does not, suggesting that anaerobic autotrophs are the main autotrophic metabolisms in this lake (in terms of DIC uptake). In La Alberca, the increase of [POC] to maximum values at depth also supports the predominance of anoxygenic *versus* oxygenic autotrophy (Fig. 3). This is similar to other stratified water bodies which exhibit primary production clearly dominated by anoxygenic metabolisms (Fulton et al., 2018).

Last, at 23 m in Lake Atexcac and 17 m in Lake La Alberca, we find a striking turbidity peak precisely where the redox potential and the concentration of dissolved Mn drops (Fig. 2). In Lake Atexcac concentrations of dissolved metal such as Cu, Pb or Co also drop at 23 m (Fig. S4). In La Alberca, a peak of particulate Mn concentrations is detected at 15 m (Fig. 2; data not available for Atexcac). This is most likely explained by the precipitation of Mn as mineral particles where reduced bottom waters meet oxidative conditions prevailing in the upper waters. These oxidized Mn phases can be used as electron acceptors during chemoautotrophy (Havig et al., 2015; Knossow et al., 2015; Henkel et al., 2019; van Vliet et al., 2021). Moreover, even at a low particle density, such phases can catalyze abiotic oxidation of sulfide to sulfur compounds (van Vliet et al., 2021), which in turn can be used and further oxidized to sulfate by phototrophic or chemoautotrophic sulfur-oxidizing bacteria. This is also consistent with the small increase of $[SO_4^{2-}]$ observed at 23 m in Atexcac (Table S2).

5.2.2. Sinks of particulate organic carbon: respiration and sedimentation

Aerobic respiration at the oxycline

At the oxycline of stratified water bodies, aerobic respiration of OM by heterotrophic organisms favors the transition from oxygenated upper layers to anoxic bottom waters. In the water column of the four lakes, $\Delta^{13}C_{POC\text{-}DIC}$ (and $\varepsilon_{POC\text{-}CO2}$) show increasing values in the hypolimnion, and especially below the chlorophyll a peaks (Figs. 2 and 5). This trend also correlates with increasing $\delta^{13}C_{POC,}$ decreasing $(C{:}N)_{POM}$ ratios as well as decreasing POC concentrations (except in La Alberca) (Figs 3 and 4). Decreasing POC concentrations near the oxycline and redoxcline are consistent with the fact that part of the upper primary production is degraded deeper in the water columns and/or that there is less primary production in the anoxic bottom waters. Increase of $\delta^{13}C_{POC}$ in the hypolimnion of the lakes is consistent with heterotrophic activity and points out that POC at these depths could mainly record secondary production rather than being residues of sinking degraded OM formed by primary production. Indeed, heterotrophic bacteria preferentially grow on available ^{13}C-enriched amino acids and sugars, thus becoming more enriched than their C source (Williams and Gordon, 1970; Hayes et al., 1989; Zohary et al., 1994; Briones et al., 1998; Lehmann et al., 2002; Jiao et al., 2010; Close and Henderson, 2020). The decrease in C:N ratios in the POM also reinforces this conclusion since secondary heterotrophic bacteria biomass generally have C:N between 4 and 5 (Lehmann et al., 2002), whereas residual degraded OM from primary producers would carry higher C:N signatures (van Mooy et al., 2002; Buchan et al., 2014). These latter signatures are not recorded by POM in the lower water columns of the lakes (Fig. 3). In Lake La Preciosa, the water column shifts from a highly oxygenated state to anoxia over a ~5 m interval against more than 10 m for Alchichica and Atexcac. This correlates with a sharp $\delta^{13}C_{POC}$ increase (+ 3.4‰), highlighting how efficient and O_2-dependent the remineralization process is in this lake.

The $\delta^{13}C_{DIC}$ signatures in lakes Alchichica and La Preciosa are consistent with the mineralization of OM as they exhibit lower values below the oxycline than in surficial waters (Figs. 2 and 4). Similarly to what is observed in several other water bodies and notably stratified water columns such as the Black Sea (*e.g.* Fry et al., 1991), surface photosynthesis increases $\delta^{13}C_{DIC}$ by fixing light DIC, while respiration transfers light OC back to the DIC pool at depth. Such a decrease of the $\delta^{13}C_{DIC}$ can also be seen in the oxycline of Lake La Alberca between 7 and 10 m.

644 *Influence of methanogenesis in Lake La Alberca de los Espinos*

645 Lake La Alberca shows the least saline/alkaline water column and most peculiar geochemical depth profiles among
646 the four lakes. Notably, its [DIC] and $\delta^{13}C_{DIC}$ (the lowest of the studied lakes) increase from the lower metalimnion
647 to the hypolimnion and further into the porewaters of the first cm of sediments with $\delta^{13}C_{DIC}$ reaching up to ~10 ‰
648 (Figs. 3; 4). Consistently, the calculated CO_2 partial pressure (P_{CO2}) increases downward from slightly less than 1x
649 that of atmospheric P_{CO2} near the lake surface up to almost 40x at the bottom of the lake (Table S1).

650 While the increase of [POC] at depth may contribute to the observed $\delta^{13}C_{DIC}$ increase by mass balance, it should
651 also lower the [DIC] instead of increasing it. Similarly, the sinking of POC at depth followed by its
652 remineralization into DIC cannot explain those observations since this would lower the $\delta^{13}C_{DIC}$ in the hypolimnion
653 (Fig. 4). Overall, these observations require that a significant source of inorganic ^{13}C-rich carbon fuels the bottom
654 waters of La Alberca de los Espinos. The source of heavy carbon most likely results from methanogenesis, which
655 consumes organic carbon in the sediments and produces ^{13}C-depleted methane and ^{13}C-rich carbon dioxide
656 diffusing upward in the water column (likely acetoclastic methanogenesis, dominant in lacustrine contexts,
657 Whiticar et al., 1986). Methanogenesis, as an "alternative" OM remineralization pathway could be favored in Lake
658 La Alberca, because this lake is relatively rich in OM (notably with high [DOC], Havas et al., submitted), and
659 depleted in SO_4^{2-} (Wittkop et al., 2014; Birgel et al., 2015; Cadeau et al., 2020) compared with the three other
660 Mexican lakes. Based on the isotopic compositions of sedimentary organic carbon and porewater DIC in Lake La
661 Alberca, we can tentatively calculate the methane isotopic signature (see supplementary text S4). The calculated
662 $\delta^{13}C_{CH4}$ in the first 10 cm of sediments is between -59 and -57 ‰, which is consistent with the range of isotopic
663 composition of methane after biogenic methanogenesis (Whiticar et al., 1986).

664 Upward diffusing methane may be either (i) partly lost from the lake's surface (*i.e.* escaping the system) by
665 degassing or (ii) totally kept in the water column by complete oxidation (either abiotically by oxygenated surface
666 waters or biologically by methanotrophic organisms). The oxidation of CH_4 in the water column should lead to the
667 formation of ^{13}C-depleted carbon dioxide that would mix back with the lake DIC (and notably with heavy
668 methanogenic CO_2 produced at depth) and/or ^{13}C-depleted biomass (as POC or SOC) if it occurs by
669 methanotrophy. Thus, the net effect of combined methanogenesis and methane oxidation is expected to (i) generate
670 a $\delta^{13}C_{DIC}$ gradient from high to low values between the sediment porewaters and the oxycline as proposed
671 elsewhere (Assayag et al., 2008; Wittkop et al., 2014) and (ii) progressively lower sedimentary $\delta^{13}C_{SOC}$ in case of
672 methanotrophy. Abiotic oxidation of methane by dioxygen is consistent with the observations that $\delta^{13}C_{DIC}$
673 decreases from porewaters (~ +10 ‰) to the oxycline (-4 ‰), reaching minimum values where dissolved-O_2 starts
674 to appear (Fig. 2). On the other hand, microbial anaerobic oxidation of methane (AOM) could occur at the 17 m
675 depth through Mn-oxides reduction (Cai et al., 2021; Cheng et al., 2021) and possibly bacterial sulfate-reduction
676 closer to the water-sediment interface, as inferred for the surficial sediments of meromictic Lake Cadagno (Posth
677 et al., 2017). Indeed, we observe a net increase of particulate Fe and S concentrations at a depth of 25 m and a
678 peak of solid sulfide minerals in the surficial sediments (Fig. S5). However, $\delta^{13}C_{SOC}$ and $\delta^{13}C_{POC}$ are far from
679 calculated $\delta^{13}C_{CH4}$, suggesting that AOM is not a major process in the bottom lake waters and surface sediments
680 (Lehmann et al., 2004) and thus that methanotrophy is not the main CH_4 oxidation pathway in Lake La Alberca.

681 Alternatively, if some portion of the methane escaped oxidation and degassed out of the lake, $\delta^{13}C_{DIC}$ would likely
682 be driven to extreme positive values with time, as observed elsewhere (Gu et al., 2004; Hassan, 2014; Birgel et al.,

683 2015; Cadeau et al., 2020). This is not consistent with the observation that the average $\delta^{13}C_{DIC}$ in Lake La Alberca
684 is about -3 ‰ (Fig. 4), unless an additional counterbalancing source of DIC to this lake exist. This source of DIC
685 could be volcanic CO_2-degassing (see section 5.1.1). Such a contribution may maintain the lake's average $\delta^{13}C_{total}$
686 close to a mantle isotopic signature and notably away from extreme positive values if CH_4-escape dominated. It is
687 also possible that volcanic CO_2 degassing is coupled to methanogenesis by CO_2 reduction in addition to the
688 acetoclastic one described above. We observe a strong pH decline at depth in this lake (mostly below 17 m, Fig. 2)
689 which could be fostered by both the acidic volcanic gases (Pecoraino et al., 2015) and methanogenesis, although
690 other redox and microbial reactions could impact the pH as well (Soetaert et al., 2007).

691 Although volcanic CO_2 could be an important source in the C mass balance of Lake La Alberca, we note that it
692 cannot explain the very positive $\delta^{13}C_{DIC}$ in the sediment porewaters alone, thus bolstering the identification of
693 methanogenesis. Only a future quantification of the fluxes of sedimentary methane production, volcanic CO_2 and
694 possible CH_4 efflux out of the lake will help to quantify the peculiar C cycle of Lake La Alberca.

695

696 *Transfer of OM from the water column to the surficial sediments*

697 The first 12 cm of the sediment cores of the four lakes contain varying quantities of OC between 1 and 13 wt. %
698 (Table 3). This appears to be relatively elevated considering the predominant autochthonous nature of OC and
699 oligotrophic conditions in these lakes (Alcocer et al., 2014; Havas et al., submitted). In Lake Alchichica, the recent
700 OC burial flux in the sediment was estimated to represent between 15 and 26 $g.yr^{-1}.m^{-2}$ (Alcocer et al., 2014). This
701 is within the range of values provided for small lakes around the world (Mulholland and Elwood, 1982; Dean and
702 Gorham, 1998; Mendonça et al., 2017), though most of them receive allochthonous OM inputs. Different factors
703 can favor the preservation of OM including lower respiration and oxidation rates due to anoxic bottom waters and
704 scarce benthic biota and/or high sedimentation rates (Alcocer et al., 2014). Anaerobic respiration clearly occurs in
705 the four lakes to some extent, as detailed for La Alberca in section 5.2.2, and as seen in the surficial sediment data
706 of the other lakes as well (decreasing $\delta^{13}C_{DIC}$ in Alchichica, increasing C:N ratio in Atexcac and La Preciosa;
707 Table 3). Nonetheless, the anoxic conditions prevailing in the hypolimnion most of the year are significantly more
708 favorable to OM preservation than oxic conditions (Sobek et al., 2009; Kuntz et al., 2015). In Alchichica, the large
709 size if phytoplankton was also suggested to favor OM preservation (Adame et al., 2008; Ardiles et al., 2011). In
710 La Alberca the low sulfate content (which is an important electron acceptor for anaerobic respiration) probably
711 favors the preservation of high TOC in the sediments. Again, a complete mass-balance of these lakes C fluxes will
712 be required to estimate their net C emission or sequestration behavior.

713 Although the nature and geochemical signatures of the OM that deposits in the bottom sediments may vary
714 throughout the year, it is interesting to infer from what part(s) of the water column surficial sedimentary OM comes
715 from during the stratified seasons. In the three lakes from the SOB, $\delta^{13}C_{SOC}$ and $(C:N)_{SOM}$ signatures of the surficial
716 sediments OM lie somewhere in between POM signatures from the upper water columns and from the hypolimnion
717 (Figs. 3, 4). More precisely, in Alchichica, top $\delta^{13}C_{SOC}$ and $(C:N)_{SOM}$ signatures (-25.7 ‰ and 10.4, respectively)
718 lie much closer to values recorded in the upper water column (~ -26.5 ‰ and 10.5, respectively) implying that the
719 upper oxygenic photosynthesis production is primarily recorded. Accordingly, it was suggested that most of the
720 phytoplankton biomass being exported was composed of diatoms (Ardiles et al., 2011). In Lake Atexcac on the

721 contrary, $\delta^{13}C_{SOC}$ and $(C:N)_{SOM}$ signatures (~ -26.8 ‰ and 8, respectively) lie closer to values recorded in the
722 hypolimnion (~ -26.5 ‰ and 6.5, respectively) suggesting that SOM records mostly the anaerobic primary
723 production.

724 In Lake La Alberca, surficial $\delta^{13}C_{SOC}$ are markedly more negative (by ~ 2 to 3 ‰) than the deepest and shallowest
725 water column values (Fig. 4) but they are close to what is recorded at the redoxcline depth of 17 m. However, the
726 $(C:N)_{SOM}$ values are much higher than what is measured anywhere in the water column, which is consistent with
727 remineralization of OM by sulfate-reduction and methanogenesis in the sediments of this lake. Therefore, OM
728 biogeochemical signatures in La Alberca's surficial sediments could be strongly influenced by early diagenesis
729 occurring at the water-sediment interface – despite favorable conditions for OM preservation. Importantly though,
730 methanogenesis/methanotrophy are recorded in the surficial sediments porewaters (notably seen through
731 extremely positive $\delta^{13}C_{DIC}$) but not in the solid sediments that show neither very negative $\delta^{13}C_{SOC}$ nor positive
732 $\delta^{13}C_{carbonates}$ in the first 10 cm.

733 Overall, this suggests that OM depositing at the bottom of these stratified lakes do not always record geochemical
734 signatures from the same parts of the water columns and can be modified by very early diagenesis. Notably, they
735 do not necessarily record the signatures of primary production by oxygenic photosynthesis from the upper column.
736 For example, in Lake Atexcac, sedimentary OM records instead primary production by anoxygenic photosynthesis,
737 even though POC concentration was maximum in the upper water column. A deeper understanding of the OM
738 transfer process from water columns to sediments will require more detailed analyses and comparison of the
739 different OM pigments and molecules and could have strong implications for interpretation of the fossil record in
740 the deep anoxic time.

741

742 **6. CONCLUSIONS AND SUMMARY**

743 The carbon cycles of four stratified alkaline crater lakes were described and compared based on the concentration
744 and isotopic compositions of DIC and POC in the water columns and of surficial (~10 cm) sedimentary carbonates
745 and organic carbon. We identify different regimes of C cycling in the four lakes due to different biogeochemical
746 reactions related to slight environmental and ecological variations. In more details, we show that:

747 - External abiotic factors, such as the hydrological regime and the inorganic C sources to the lakes, control
748 their alkalinity and thus, the buffering capacities of their waters. In turn, it constrains the stratification of
749 the water columns and the inorganic C isotopic signatures of the lakes water columns and sediments.
750 Furthermore, it impacts the C mass balance of the lakes with probable consequences on their net C-
751 emitting or -sequestering status.
752 - Based on POC and DIC concentrations and isotopic compositions, combined with physico-chemical
753 parameters, we are able to identify the activity of oxygenic photosynthesis and aerobic respiration in the
754 four studied lakes. Anoxygenic photosynthesis and/or chemoautotrophy are also evidenced in some of
755 the lakes, but their POC and DIC signatures can be equivocal.
756 - Methanogenesis is evidenced in the surficial sediments of the OM-rich Lake La Alberca de los Espinos
757 and influences the lower water column geochemical signatures. However, it is recorded only by analyses
758 of porewater dissolved species, but not imprinted in the sedimentary archives (solid OM and carbonates).

- Last, we observe that the SOM geochemical signatures of these stratified lakes do not all record the same "biogeochemical layers" of the water column and can be largely modified by early diagenesis in some cases. Meanwhile, most carbonate phases in bottom lake sediments are in isotopic equilibrium with lake oxyclines, while some might be detrital in origin.

Author Contributions

RH and CT designed the study in a project directed by PLG, KB and CT. CT, MI, DJ, DM, RT, PLG and KB collected the samples on the field. RH carried out the measurements for C data; DJ the physico-chemical parameter probe measurements and EM provided data for trace and major elements. RH and CT analyzed the data. RH wrote the manuscript with important contributions of all co-authors.

Competing Interests

The authors declare that they have no conflict of interest.

Disclaimer

Acknowledgements

This work was supported by Agence Nationale de la Recherche (France; ANR Microbialites, grant number ANR-18-CE02-0013-02). The authors thank Anne-Lise Santoni, Elodie Cognard, Théophile Cocquerez and the GISMO platform (Biogéosciences, Université Bourgogne Franche-Comté, UMR CNRS 6282, France). We thank Céline Liorzou and Bleuenn Guéguen for the analyses at the Pôle Spectrométrie Océan (Laboratoire Géo-Océan, Brest, France) and Laure Cordier for ion chromatography analyses at IPGP (France). We thank Nelly Assayag and Pierre Cadeau for their help on the AP 2003 at IPGP.

References

Adame, M.F., Alcocer, J., Escobar, E., 2008. Size-fractionated phytoplankton biomass and its implications for the dynamics of an oligotrophic tropical lake. Freshw. Biol. 53, 22–31. https://doi.org/10.1111/j.1365-2427.2007.01864.x

Alcocer, J., 2021. Lake Alchichica Limnology, Springer Nature. ed.

Alcocer, J., Ruiz-Fernández, A.C., Escobar, E., Pérez-Bernal, L.H., Oseguera, L.A., Ardiles-Gloria, V., 2014. Deposition, burial and sequestration of carbon in an oligotrophic, tropical lake. J. Limnol. 73. https://doi.org/10.4081/jlimnol.2014.783

Anderson, N.John., Stedmon, C.A., 2007. The effect of evapoconcentration on dissolved organic carbon concentration and quality in lakes of SW Greenland. Freshw. Biol. 52, 280–289. https://doi.org/10.1111/j.1365-2427.2006.01688.x

Ardiles, V., Alcocer, J., Vilaclara, G., Oseguera, L.A., Velasco, L., 2012. Diatom fluxes in a tropical, oligotrophic lake dominated by large-sized phytoplankton. Hydrobiologia 679, 77–90. https://doi.org/10.1007/s10750-011-0853-7

Armienta, M.A., Vilaclara, G., De la Cruz-Reyna, S., Ramos, S., Ceniceros, N., Cruz, O., Aguayo, A., Arcega-Cabrera, F., 2008. Water chemistry of lakes related to active and inactive Mexican volcanoes. J. Volcanol. Geotherm. Res. 178, 249–258. https://doi.org/10.1016/j.jvolgeores.2008.06.019

Armstrong-Altrin, J.S., Madhavaraju, J., Sial, A.N., Kasper-Zubillaga, J.J., Nagarajan, R., Flores-Castro, K., Rodríguez, J.L., 2011. Petrography and stable isotope geochemistry of the cretaceous El Abra Limestones (Actopan), Mexico: Implication on diagenesis. J. Geol. Soc. India 77, 349–359. https://doi.org/10.1007/s12594-011-0042-3

Assayag, N., Jézéquel, D., Ader, M., Viollier, E., Michard, G., Prévot, F., Agrinier, P., 2008. Hydrological budget, carbon sources and biogeochemical processes in Lac Pavin (France): Constraints from δ18O of water and δ13C of dissolved inorganic carbon. Appl. Geochem. 23, 2800–2816. https://doi.org/10.1016/j.apgeochem.2008.04.015

Assayag, N., Rivé, K., Ader, M., Jézéquel, D., Agrinier, P., 2006. Improved method for isotopic and quantitative analysis of dissolved inorganic carbon in natural water samples. Rapid Commun. Mass Spectrom. 20, 2243–2251. https://doi.org/10.1002/rcm.2585

Bade, D.L., Carpenter, S.R., Cole, J.J., Hanson, P.C., Hesslein, R.H., 2004. Controls of δ13C-DIC in lakes: Geochemistry, lake metabolism, and morphometry. Limnol. Oceanogr. 49, 1160–1172. https://doi.org/10.4319/lo.2004.49.4.1160

Bekker, A., Holmden, C., Beukes, N.J., Kenig, F., Eglinton, B., Patterson, W.P., 2008. Fractionation between inorganic and organic carbon during the Lomagundi (2.22–2.1 Ga) carbon isotope excursion. Earth Planet. Sci. Lett. 271, 278–291. https://doi.org/10.1016/j.epsl.2008.04.021

Birgel, D., Meister, P., Lundberg, R., Horath, T.D., Bontognali, T.R.R., Bahniuk, A.M., de Rezende, C.E., Vasconcelos, C., McKenzie, J.A., 2015. Methanogenesis produces strong 13C enrichment in stromatolites of Lagoa Salgada, Brazil: a modern analogue for Palaeo-/Neoproterozoic stromatolites? Geobiology 13, 245–266. https://doi.org/10.1111/gbi.12130

Briones, E.E., Alcocer, J., Cienfuegos, E., Morales, P., 1998. Carbon stable isotopes ratios of pelagic and littoral communities in Alchichica crater-lake, Mexico. Int. J. Salt Lake Res. 7, 345–355. https://doi.org/10.1007/BF02442143

Buchan, A., LeCleir, G.R., Gulvik, C.A., González, J.M., 2014. Master recyclers: features and functions of bacteria associated with phytoplankton blooms. Nat. Rev. Microbiol. 12, 686–698. https://doi.org/10.1038/nrmicro3326

Cadeau, P., Jézéquel, D., Leboulanger, C., Fouilland, E., Le Floc'h, E., Chaduteau, C., Milesi, V., Guélard, J., Sarazin, G., Katz, A., d'Amore, S., Bernard, C., Ader, M., 2020. Carbon isotope evidence for large methane emissions to the Proterozoic atmosphere. Sci. Rep. 10, 18186. https://doi.org/10.1038/s41598-020-75100-x

Cai, C., Li, K., Liu, D., John, C.M., Wang, D., Fu, B., Fakhraee, M., He, H., Feng, L., Jiang, L., 2021. Anaerobic oxidation of methane by Mn oxides in sulfate-poor environments. Geology 49, 761–766. https://doi.org/10.1130/G48553.1

Callieri, C., Coci, M., Corno, G., Macek, M., Modenutti, B., Balseiro, E., Bertoni, R., 2013. Phylogenetic diversity of nonmarine picocyanobacteria. FEMS Microbiol. Ecol. 85, 293–301. https://doi.org/10.1111/1574-6941.12118

Camacho, A., Walter, X.A., Picazo, A., Zopfi, J., 2017. Photoferrotrophy: Remains of an Ancient Photosynthesis in Modern Environments. Front. Microbiol. 08. https://doi.org/10.3389/fmicb.2017.00323

Carrasco-Núñez, G., Ort, M.H., Romero, C., 2007. Evolution and hydrological conditions of a maar volcano (Atexcac crater, Eastern Mexico). J. Volcanol. Geotherm. Res. 159, 179–197. https://doi.org/10.1016/j.jvolgeores.2006.07.001

Chako Tchamabé, B., Carrasco-Núñez, G., Miggins, D.P., Németh, K., 2020. Late Pleistocene to Holocene activity of Alchichica maar volcano, eastern Trans-Mexican Volcanic Belt. J. South Am. Earth Sci. 97, 102404. https://doi.org/10.1016/j.jsames.2019.102404

Cheng, C., Zhang, J., He, Q., Wu, H., Chen, Y., Xie, H., Pavlostathis, S.G., 2021. Exploring simultaneous nitrous oxide and methane sink in wetland sediments under anoxic conditions. Water Res. 194, 116958. https://doi.org/10.1016/j.watres.2021.116958

Close, H.G., Henderson, L.C., 2020. Open-Ocean Minima in δ13C Values of Particulate Organic Carbon in the Lower Euphotic Zone. Front. Mar. Sci. 7, 540165. https://doi.org/10.3389/fmars.2020.540165

Crowe, S.A., Katsev, S., Leslie, K., Sturm, A., Magen, C., Nomosatryo, S., Pack, M.A., Kessler, J.D., Reeburgh, W.S., Roberts, J.A., González, L., Douglas Haffner, G., Mucci, A., Sundby, B., Fowle, D.A., 2011. The methane cycle in ferruginous Lake Matano: Methane cycle in ferruginous Lake Matano. Geobiology 9, 61–78. https://doi.org/10.1111/j.1472-4669.2010.00257.x

Dean, W.E., Gorham, E., 1998. Magnitude and significance of carbon burial in lakes, reservoirs, and peatlands. Geology 26, 535. https://doi.org/10.1130/0091-7613(1998)026<0535:MASOCB>2.3.CO;2

Descolas-Gros, C., Fontungne, M., 1990. Stable carbon isotope fractionation by marine phytoplankton during photosynthesis. Plant Cell Environ. 13, 207–218. https://doi.org/10.1111/j.1365-3040.1990.tb01305.x

Emrich, K., Ehhalt, D.H., Vogel, J.C., 1970. Carbon isotope fractionation during the precipitation of calcium carbonate. Earth Planet. Sci. Lett. 8, 363–371. https://doi.org/10.1016/0012-821X(70)90109-3

Ferrari, L., Orozco-Esquivel, T., Manea, V., Manea, M., 2012. The dynamic history of the Trans-Mexican Volcanic Belt and the Mexico subduction zone. Tectonophysics 522–523, 122–149. https://doi.org/10.1016/j.tecto.2011.09.018

Fogel, M.L., Cifuentes, L.A., 1993. Isotope Fractionation during Primary Production, in: Engel, M.H., Macko, S.A. (Eds.), Organic Geochemistry, Topics in Geobiology. Springer US, Boston, MA, pp. 73–98. https://doi.org/10.1007/978-1-4615-2890-6_3

Fry, B., 2021. 13C/12C fractionation by marine diatoms 13.

Fry, B., Jannasch, H.W., Molyneaux, S.J., Wirsen, C.O., Muramoto, J.A., King, S., 1991. Stable isotope studies of the carbon, nitrogen and sulfur cycles in the Black Sea and the Cariaco Trench. Deep Sea Res. Part Oceanogr. Res. Pap. 38, S1003–S1019. https://doi.org/10.1016/S0198-0149(10)80021-4

Fulton, J.M., Arthur, M.A., Thomas, B., Freeman, K.H., 2018. Pigment carbon and nitrogen isotopic signatures in euxinic basins. Geobiology 16, 429–445. https://doi.org/10.1111/gbi.12285

Furian, S., Martins, E.R.C., Parizotto, T.M., Rezende-Filho, A.T., Victoria, R.L., Barbiero, L., 2013. Chemical diversity and spatial variability in myriad lakes in Nhecolândia in the Pantanal wetlands of Brazil. Limnol. Oceanogr. 58, 2249–2261. https://doi.org/10.4319/lo.2013.58.6.2249

Gérard, E., Ménez, B., Couradeau, E., Moreira, D., Benzerara, K., Tavera, R., López-García, P., 2013. Specific carbonate–microbe interactions in the modern microbialites of Lake Alchichica (Mexico). ISME J. 7, 1997–2009. https://doi.org/10.1038/ismej.2013.81

Gonzales-Partida, E., Barragan-R, R.M., Nieva-G, D., 1993. Analisis geoquimico-isotopico de las especies carbonicas del fluido geotermico de Los Humeros, Puebla, México. Geofis. Int. 32, 299–309.

Gröger, J., Franke, J., Hamer, K., Schulz, H.D., 2009. Quantitative Recovery of Elemental Sulfur and Improved Selectivity in a Chromium-Reducible Sulfur Distillation. Geostand. Geoanalytical Res. 33, 17–27. https://doi.org/10.1111/j.1751-908X.2009.00922.x

Gu, B., Schelske, C.L., Hodell, D.A., 2004. Extreme13C enrichments in a shallow hypereutrophic lake: Implications for carbon cycling. Limnol. Oceanogr. 49, 1152–1159. https://doi.org/10.4319/lo.2004.49.4.1152

Hassan, K.M., 2014. Isotope geochemistry of Swan Lake Basin in the Nebraska Sandhills, USA: Large 13C enrichment in sediment-calcite records. Geochemistry 74, 681–690. https://doi.org/10.1016/j.chemer.2014.03.004

Havig, J.R., Hamilton, T.L., McCormick, M., McClure, B., Sowers, T., Wegter, B., Kump, L.R., 2018. Water column and sediment stable carbon isotope biogeochemistry of permanently redox- stratified Fayetteville Green Lake, New York, U.S.A. Limnol. Oceanogr. 63, 570–587. https://doi.org/10.1002/lno.10649

Havig, J.R., McCormick, M.L., Hamilton, T.L., Kump, L.R., 2015. The behavior of biologically important trace elements across the oxic/euxinic transition of meromictic Fayetteville Green Lake, New York, USA. Geochim. Cosmochim. Acta 165, 389–406. https://doi.org/10.1016/j.gca.2015.06.024

Hayes, J.M., Popp, B.N., Takigiku, R., Johnson, M.W., 1989. An isotopic study of biogeochemical relationships between carbonates and organic carbon in the Greenhorn Formation. Geochim. Cosmochim. Acta 53, 2961–2972. https://doi.org/10.1016/0016-7037(89)90172-5

Henkel, J.V., Dellwig, O., Pollehne, F., Herlemann, D.P.R., Leipe, T., Schulz-Vogt, H.N., 2019. A bacterial isolate from the Black Sea oxidizes sulfide with manganese(IV) oxide. Proc. Natl. Acad. Sci. 116, 12153–12155. https://doi.org/10.1073/pnas.1906000116

Hessen, D.O., Anderson, T.R., 2008. Excess carbon in aquatic organisms and ecosystems: Physiological, ecological, and evolutionary implications. Limnol. Oceanogr. 53, 1685–1696. https://doi.org/10.4319/lo.2008.53.4.1685

Hurley, S.J., Wing, B.A., Jasper, C.E., Hill, N.C., Cameron, J.C., 2021. Carbon isotope evidence for the global physiology of Proterozoic cyanobacteria. Sci. Adv. 7, eabc8998. https://doi.org/10.1126/sciadv.abc8998

Iniesto, M., Moreira, D., Benzerara, K., Muller, E., Bertolino, P., Tavera, R., López- García, P., 2021a. Rapid formation of mature microbialites in Lake Alchichica, Mexico. Environ. Microbiol. Rep. 13, 600–605. https://doi.org/10.1111/1758-2229.12957

Iniesto, M., Moreira, D., Benzerara, K., Reboul, G., Bertolino, P., Tavera, R., López- García, P., 2022. Planktonic microbial communities from microbialite- bearing lakes sampled along a salinity- alkalinity gradient. Limnol. Oceanogr. lno.12233. https://doi.org/10.1002/lno.12233

Iniesto, M., Moreira, D., Reboul, G., Deschamps, P., Benzerara, K., Bertolino, P., Saghaï, A., Tavera, R., López- García, P., 2021b. Core microbial communities of lacustrine microbialites sampled along an alkalinity gradient. Environ. Microbiol. 23, 51–68. https://doi.org/10.1111/1462-2920.15252

Iñiguez, C., Capó- Bauçà, S., Niinemets, Ü., Stoll, H., Aguiló- Nicolau, P., Galmés, J., 2020. Evolutionary trends in RuBisCO kinetics and their co- evolution with CO2 concentrating mechanisms. Plant J. 101, 897–918. https://doi.org/10.1111/tpj.14643

Javoy, M., Pineau, F., Delorme, H., 1986. Carbon and nitrogen isotopes in the mantle. Chem. Geol., Isotopes in Geology—Picciotto Volume 57, 41–62. https://doi.org/10.1016/0009-2541(86)90093-8

Jézéquel, D., Michard, G., Viollier, E., Agrinier, P., Albéric, P., Lopes, F., Abril, G., Bergonzini, L., 2016. Carbon Cycle in a Meromictic Crater Lake: Lake Pavin, France, in: Sime-Ngando, T., Boivin, P., Chapron, E., Jezequel, D., Meybeck, M. (Eds.), Lake Pavin: History, Geology, Biogeochemistry, and Sedimentology of a Deep Meromictic Maar Lake. Springer International Publishing, Cham, pp. 185–203. https://doi.org/10.1007/978-3-319-39961-4_11

Jiao, N., Herndl, G.J., Hansell, D.A., Benner, R., Kattner, G., Wilhelm, S.W., Kirchman, D.L., Weinbauer, M.G., Luo, T., Chen, F., Azam, F., 2010. Microbial production of recalcitrant dissolved organic matter: long-term carbon storage in the global ocean. Nat. Rev. Microbiol. 8, 593–599. https://doi.org/10.1038/nrmicro2386

Karhu, J.A., Holland, H.D., 1996. Carbon isotopes and the rise of atmospheric oxygen. Geology 24, 867. https://doi.org/10.1130/0091-7613(1996)024<0867:CIATRO>2.3.CO;2

Klawonn, I., Van den Wyngaert, S., Parada, A.E., Arandia-Gorostidi, N., Whitehouse, M.J., Grossart, H.-P., Dekas, A.E., 2021. Characterizing the "fungal shunt": Parasitic fungi on diatoms affect carbon flow and bacterial communities in aquatic microbial food webs. Proc. Natl. Acad. Sci. 118, e2102225118. https://doi.org/10.1073/pnas.2102225118

Knossow, N., Blonder, B., Eckert, W., Turchyn, A.V., Antler, G., Kamyshny, A., 2015. Annual sulfur cycle in a warm monomictic lake with sub-millimolar sulfate concentrations. Geochem. Trans. 16, 7. https://doi.org/10.1186/s12932-015-0021-5

Kuntz, L.B., Laakso, T.A., Schrag, D.P., Crowe, S.A., 2015. Modeling the carbon cycle in Lake Matano. Geobiology 13, 454–461. https://doi.org/10.1111/gbi.12141

Lehmann, M.F., Bernasconi, S.M., Barbieri, A., McKenzie, J.A., 2002. Preservation of organic matter and alteration of its carbon and nitrogen isotope composition during simulated and in situ early sedimentary diagenesis. Geochim. Cosmochim. Acta 66, 3573–3584. https://doi.org/10.1016/S0016-7037(02)00968-7

Lehmann, M.F., Bernasconi, S.M., McKenzie, J.A., Barbieri, A., Simona, M., Veronesi, M., 2004. Seasonal variation of the δC and δN of particulate and dissolved carbon and nitrogen in Lake Lugano: Constraints on biogeochemical cycling in a eutrophic lake. Limnol. Oceanogr. 49, 415–429. https://doi.org/10.4319/lo.2004.49.2.0415

Lelli, M., Kretzschmar, T.G., Cabassi, J., Doveri, M., Sanchez-Avila, J.I., Gherardi, F., Magro, G., Norelli, F., 2021. Fluid geochemistry of the Los Humeros geothermal field (LHGF - Puebla, Mexico): New constraints for the conceptual model. Geothermics 90, 101983. https://doi.org/10.1016/j.geothermics.2020.101983

Li, H.-C., Ku, T.-L., 1997. δ13C–δ18C covariance as a paleohydrological indicator for closed-basin lakes. Palaeogeogr. Palaeoclimatol. Palaeoecol. 133, 69–80. https://doi.org/10.1016/S0031-0182(96)00153-8

Lorenz, V., 1986. On the growth of maars and diatremes and its relevance to the formation of tuff rings. Bull. Volcanol. 48, 265–274. https://doi.org/10.1007/BF01081755

Lugo, A., Alcocer, J., Sánchez, Ma. del R., Escobar, E., Macek, M., 2000. Temporal and spatial variation of bacterioplankton abundance in a tropical, warm-monomictic, saline lake: Alchichica, Puebla, Mexico. SIL Proc. 1922-2010 27, 2968–2971. https://doi.org/10.1080/03680770.1998.11898217

Lugo, A., Alcocer, J., Sanchez, M.R., Escobar, E., 1993. Trophic status of tropical lakes indicated by littoral protozoan assemblages. SIL Proc. 1922-2010 25, 441–443. https://doi.org/10.1080/03680770.1992.11900159

Lyons, T.W., Reinhard, C.T., Planavsky, N.J., 2014. The rise of oxygen in Earth's early ocean and atmosphere. Nature 506, 307–315. https://doi.org/10.1038/nature13068

Macek, M., Medina, X.S., Picazo, A., Peštová, D., Reyes, F.B., Hernández, J.R.M., Alcocer, J., Ibarra, M.M., Camacho, A., 2020. Spirostomum teres: A Long Term Study of an Anoxic-Hypolimnion Population Feeding upon Photosynthesizing Microorganisms. Acta Protozool. 59, 13–38. https://doi.org/10.4467/16890027AP.20.002.12158

Mason, E., Edmonds, M., Turchyn, A.V., 2017. Remobilization of crustal carbon may dominate volcanic arc emissions. Science 357, 290–294. https://doi.org/10.1126/science.aan5049

Mendonça, R., Müller, R.A., Clow, D., Verpoorter, C., Raymond, P., Tranvik, L.J., Sobek, S., 2017. Organic carbon burial in global lakes and reservoirs. Nat. Commun. 8, 1694. https://doi.org/10.1038/s41467-017-01789-6

Mercedes-Martín, R., Ayora, C., Tritlla, J., Sánchez-Román, M., 2019. The hydrochemical evolution of alkaline volcanic lakes: a model to understand the South Atlantic Pre-salt mineral assemblages. Earth-Sci. Rev. 198, 102938. https://doi.org/10.1016/j.earscirev.2019.102938

Milesi, V.P., Debure, M., Marty, N.C.M., Capano, M., Jézéquel, D., Steefel, C., Rouchon, V., Albéric, P., Bard, E., Sarazin, G., Guyot, F., Virgone, A., Gaucher, É.C., Ader, M., 2020. Early Diagenesis of Lacustrine Carbonates in Volcanic Settings: The Role of Magmatic CO_2 (Lake Dziani Dzaha, Mayotte, Indian Ocean). ACS Earth Space Chem. 4, 363–378. https://doi.org/10.1021/acsearthspacechem.9b00279

Mook, W.G., Bommerson, J.C., Staverman, W.H., 1974. Carbon isotope fractionation between dissolved bicarbonate and gaseous carbon dioxide. Earth Planet. Sci. Lett. 22, 169–176. https://doi.org/10.1016/0012-821X(74)90078-8

Mulholland, P.J., Elwood, J.W., 1982. The role of lake and reservoir sediments as sinks in the perturbed global carbon cycle. Tellus 34, 490–499. https://doi.org/10.1111/j.2153-3490.1982.tb01837.x

O'Leary, M.H., 1988. Carbon Isotopes in Photosynthesis. BioScience 38, 328–336. https://doi.org/10.2307/1310735

Paneth, P., O'Leary, M.H., 1985. Carbon isotope effect on dehydration of bicarbonate ion catalyzed by carbonic anhydrase. Biochemistry 24, 5143–5147. https://doi.org/10.1021/bi00340a028

Pardue, J.W., Scalan, R.S., Van Baalen, C., Parker, P.L., 1976. Maximum carbon isotope fractionation in photosynthesis by blue-green algae and a green alga. Geochim. Cosmochim. Acta 40, 309–312. https://doi.org/10.1016/0016-7037(76)90208-8

Pecoraino, G., D'Alessandro, W., Inguaggiato, S., 2015. The Other Side of the Coin: Geochemistry of Alkaline Lakes in Volcanic Areas, in: Rouwet, D., Christenson, B., Tassi, F., Vandemeulebrouck, J. (Eds.), Volcanic Lakes, Advances in Volcanology. Springer Berlin Heidelberg, Berlin, Heidelberg, pp. 219–237. https://doi.org/10.1007/978-3-642-36833-2_9

Peiffer, L., Carrasco-Núñez, G., Mazot, A., Villanueva-Estrada, R.E., Inguaggiato, C., Bernard Romero, R., Rocha Miller, R., Hernández Rojas, J., 2018. Soil degassing at the Los Humeros geothermal field (Mexico). J. Volcanol. Geotherm. Res. 356, 163–174. https://doi.org/10.1016/j.jvolgeores.2018.03.001

Petrash, D.A., Steenbergen, I.M., Valero, A., Meador, T.B., Pačes, T., Thomazo, C., 2022. Aqueous system-level processes and prokaryote assemblages in the ferruginous and sulfate-rich bottom waters of a post-mining lake. Biogeosciences 19, 1723–1751. https://doi.org/10.5194/bg-19-1723-2022

Pimenov, N.V., Lunina, O.N., Prusakova, T.S., Rusanov, I.I., Ivanov, M.V., 2008. Biological fractionation of stable carbon isotopes at the aerobic/anaerobic water interface of meromictic water bodies. Microbiology 77, 751–759. https://doi.org/10.1134/S0026261708060131

Posth, N.R., Bristow, L.A., Cox, R.P., Habicht, K.S., Danza, F., Tonolla, M., Frigaard, N. - U., Canfield, D.E., 2017. Carbon isotope fractionation by anoxygenic phototrophic bacteria in euxinic Lake Cadagno. Geobiology 15, 798–816. https://doi.org/10.1111/gbi.12254

Rendon-Lopez, M.J., 2008. Limnologia fisica del lago crater los Espinos, Municipio de Jiménez Michoacan.

Ridgwell, A., Arndt, S., 2015. Chapter 1 - Why Dissolved Organics Matter: DOC in Ancient Oceans and Past Climate Change, in: Hansell, D.A., Carlson, C.A. (Eds.), Biogeochemistry of Marine Dissolved Organic Matter (Second Edition). Academic Press, Boston, pp. 1–20. https://doi.org/10.1016/B978-0-12-405940-5.00001-7

Sackett, W.M., Eckelmann, W.R., Bender, M.L., Bé, A.W.H., 1965. Temperature Dependence of Carbon Isotope Composition in Marine Plankton and Sediments. Science 148, 235–237. https://doi.org/10.1126/science.148.3667.235

Saghaï, A., Zivanovic, Y., Moreira, D., Benzerara, K., Bertolino, P., Ragon, M., Tavera, R., López-Archilla, A.I., López-García, P., 2016. Comparative metagenomics unveils functions and genome features of microbialite-associated communities along a depth gradient: Comparative metagenomics of microbialites from Lake Alchichica. Environ. Microbiol. 18, 4990–5004. https://doi.org/10.1111/1462-2920.13456

Saini, J.S., Hassler, C., Cable, R., Fourquez, M., Danza, F., Roman, S., Tonolla, M., Storelli, N., Jacquet, S., Zdobnov, E.M., Duhaime, M.B., 2021. Microbial loop of a Proterozoic ocean analogue (preprint). Microbiology. https://doi.org/10.1101/2021.08.17.456685

Satkoski, A.M., Beukes, N.J., Li, W., Beard, B.L., Johnson, C.M., 2015. A redox-stratified ocean 3.2 billion years ago. Earth Planet. Sci. Lett. 430, 43–53. https://doi.org/10.1016/j.epsl.2015.08.007

Schidlowski, M., 2001. Carbon isotopes as biogeochemical recorders of life over 3.8 Ga of Earth history: evolution of a concept. Precambrian Res. 106, 117–134. https://doi.org/10.1016/S0301-9268(00)00128-5

Schiff, S.L., Tsuji, J.M., Wu, L., Venkiteswaran, J.J., Molot, L.A., Elgood, R.J., Paterson, M.J., Neufeld, J.D., 2017. Millions of Boreal Shield Lakes can be used to Probe Archaean Ocean Biogeochemistry. Sci. Rep. 7, 46708. https://doi.org/10.1038/srep46708

Siebe, C., Guilbaud, M.-N., Salinas, S., Chédeville-Monzo, C., 2012. Eruption of Alberca de los Espinos tuff cone causes transgression of Zacapu lake ca. 25,000 yr BP in Michoacán, México. Presented at the IAS 4IMC Conference, Auckland, New Zeland, pp. 74–75.

Siebe, C., Guilbaud, M.-N., Salinas, S., Kshirsagar, P., Chevrel, M.O., Jiménez, A.H., Godínez, L., 2014. Monogenetic volcanism of the Michoacán-Guanajuato Volcanic Field: Maar craters of the Zacapu basin and domes, shields, and scoria cones of the Tarascan highlands (Paracho-Paricutin region). Presented at the Pre-meeting field guide for the 5th international Maar Conference, Querétaro, México, pp. 1–37.

Sigala, I., Caballero, M., Correa-Metrio, A., Lozano-García, S., Vázquez, G., Pérez, L., Zawisza, E., 2017. Basic limnology of 30 continental waterbodies of the Transmexican Volcanic Belt across climatic and environmental gradients. Bol. Soc. Geológica Mex. 69, 313–370. https://doi.org/10.18268/BSGM2017v69n2a3

Silva Aguilera, R.A., 2019. Analisis del descenso del nivel de agua del lago Alchichica, Puebla, México 120.

Sirevag, R., Buchanan, B.B., Berry, J.A., Troughton, J.H., 1977. Mechanisms of C02 Fixation in Bacterial Photosynthesis Studied by the Carbon Isotope Fractionation Technique. Arch Microbiol 112, 4.

Sobek, S., Durisch-Kaiser, E., Zurbrügg, R., Wongfun, N., Wessels, M., Pasche, N., Wehrli, B., 2009. Organic carbon burial efficiency in lake sediments controlled by oxygen exposure time and sediment source. Limnol. Oceanogr. 54, 2243–2254. https://doi.org/10.4319/lo.2009.54.6.2243

Soetaert, K., Hofmann, A.F., Middelburg, J.J., Meysman, F.J.R., Greenwood, J., 2007. The effect of biogeochemical processes on pH. Mar. Chem. 105, 30–51. https://doi.org/10.1016/j.marchem.2006.12.012

Talbot, M.R., 1990. A review of the palaeohydrological interpretation of carbon and oxygen isotopic ratios in primary lacustrine carbonates. Chem. Geol. Isot. Geosci. Sect. 80, 261–279. https://doi.org/10.1016/0168-9622(90)90009-2

Thomas, P.J., Boller, A.J., Satagopan, S., Tabita, F.R., Cavanaugh, C.M., Scott, K.M., 2019. Isotope discrimination by form IC RubisCO from *Ralstonia eutropha* and *Rhodobacter sphaeroides* , metabolically versatile members of ‘ *Proteobacteria* ’ from aquatic and soil habitats. Environ. Microbiol. 21, 72–80. https://doi.org/10.1111/1462-2920.14423

Ussiri, D.A.N., Lal, R., 2017. Carbon Sequestration for Climate Change Mitigation and Adaptation. Springer International Publishing, Cham. https://doi.org/10.1007/978-3-319-53845-7

Van Mooy, B.A.S., Keil, R.G., Devol, A.H., 2002. Impact of suboxia on sinking particulate organic carbon: Enhanced carbon flux and preferential degradation of amino acids via denitrification. Geochim. Cosmochim. Acta 66, 457–465. https://doi.org/10.1016/S0016-7037(01)00787-6

Vilaclara, G., Chávez, M., Lugo, A., González, H., Gaytán, M., 1993. Comparative description of crater-lakes basic chemistry in Puebla State, Mexico. SIL Proc. 1922-2010 25, 435–440. https://doi.org/10.1080/03680770.1992.11900158

Vliet, D.M., Meijenfeldt, F.A.B., Dutilh, B.E., Villanueva, L., Sinninghe Damsté, J.S., Stams, A.J.M., Sánchez-Andrea, I., 2021. The bacterial sulfur cycle in expanding dysoxic and euxinic marine waters. Environ. Microbiol. 23, 2834–2857. https://doi.org/10.1111/1462-2920.15265

Wang, S., Yeager, K.M., Lu, W., 2016. Carbon isotope fractionation in phytoplankton as a potential proxy for pH rather than for [CO2(aq)]: Observations from a carbonate lake. Limnol. Oceanogr. 61, 1259–1270. https://doi.org/10.1002/lno.10289

Werne, J.P., Hollander, D.J., 2004. Balancing supply and demand: controls on carbon isotope fractionation in the Cariaco Basin (Venezuela) Younger Dryas to present. Mar. Chem. 92, 275–293. https://doi.org/10.1016/j.marchem.2004.06.031

Whiticar, M.J., Faber, E., Schoell, M., 1986. Biogenic methane formation in marine and freshwater environments: CO2 reduction vs. acetate fermentation—Isotope evidence. Geochim. Cosmochim. Acta 50, 693–709. https://doi.org/10.1016/0016-7037(86)90346-7

Williams, P.M., Gordon, L.I., 1970. Carbon-13: carbon-12 ratios in dissolved and particulate organic matter in the sea. Deep Sea Res. Oceanogr. Abstr. 17, 19–27. https://doi.org/10.1016/0011-7471(70)90085-9

Wittkop, C., Teranes, J., Lubenow, B., Dean, W.E., 2014. Carbon- and oxygen-stable isotopic signatures of methanogenesis, temperature, and water column stratification in Holocene siderite varves. Chem. Geol. 389, 153–166. https://doi.org/10.1016/j.chemgeo.2014.09.016

Zeyen, N., Benzerara, K., Beyssac, O., Daval, D., Muller, E., Thomazo, C., Tavera, R., López-García, P., Moreira, D., Duprat, E., 2021. Integrative analysis of the mineralogical and chemical composition of modern microbialites from ten Mexican lakes: What do we learn about their formation? Geochim. Cosmochim. Acta 305, 148–184. https://doi.org/10.1016/j.gca.2021.04.030

Zohary, T., Erez, J., Gophen, M., Berman-Frank, I., Stiller, M., 1994. Seasonality of stable carbon isotopes within the pelagic food web of Lake Kinneret. Limnol. Oceanogr. 39, 1030–1043. https://doi.org/10.4319/lo.1994.39.5.1030

Zyakun, A.M., Lunina, O.N., Prusakova, T.S., Pimenov, N.V., Ivanov, M.V., 2009. Fractionation of stable carbon isotopes by photoautotrophically growing anoxygenic purple and green sulfur bacteria. Microbiology 78, 757–768. https://doi.org/10.1134/S0026261709060137